bioRxiv preprint doi: https://doi.org/10.1101/701664; this version posted July 13, 2019. The copyright holder for this preprint (which was not certified by peer review) is the author/funder, who has granted bioRxiv a license to display the preprint in perpetuity. It is made available under aCC-BY 4.0 International license.

Presynaptic Gα$_o$ (GOA-1) signaling depresses command neuron excitability to allow for stretch-dependent modulation of egg-laying behavior in *C. elegans*

Bhavya Ravi[1,2,3], Jian Zhao[4,5], Sana Chaudhry[2], Mattingly Bartole[1,2], Christian Guijarro[2,6], Lijun Kang[4], and Kevin M. Collins[1,2,7]

[1]Neuroscience Program, University of Miami Miller School of Medicine, Miami, FL USA

[2]Department of Biology, University of Miami, Coral Gables, FL USA

[3]Present address: Department of Neurology, Johns Hopkins University School of Medicine, Baltimore, MD USA

[4]Department of Neuroscience, Zhejiang University School of Medicine, Hangzhou, Zhejiang, China

[5]Present address: Department of Molecular Biology, Massachusetts General Hospital, Boston, MA USA

[6]Present address: ALPS Electric Europe GmbH, Munich, Germany

[7]To whom correspondence should be addressed:

kevin.collins@miami.edu
Department of Biology
University of Miami
1301 Memorial Drive
Coral Gables, FL 33143
Tel: (305) 284-9058

61 pages with 7 Figures, 2 Supplemental Figures, 2 Tables, and 9 Videos

Abstract- 150 words, Introduction- 1430 words, Discussion- 1877 words.

bioRxiv preprint doi: https://doi.org/10.1101/701664; this version posted July 13, 2019. The copyright holder for this preprint (which was not certified by peer review) is the author/funder, who has granted bioRxiv a license to display the preprint in perpetuity. It is made available under aCC-BY 4.0 International license.

Abstract

Caenorhabditis elegans egg laying is a two-state behavior modulated by sensory input. Feedback of egg accumulation in the uterus drives activity of the serotonergic HSN command neurons to promote the active state, but how aversive sensory stimuli signal to inhibit egg laying is not well understood. We find the Pertussis Toxin-sensitive G protein, $G\alpha_o$, signals in HSN to inhibit circuit activity and prolong the inactive behavior state. $G\alpha_o$ signaling hyperpolarizes HSN, reducing Ca^{2+} activity and input into the postsynaptic vulval muscles. Loss of inhibitory $G\alpha_o$ signaling uncouples presynaptic HSN activity from a postsynaptic, stretch-dependent homeostat, causing precocious entry into the egg-laying active state. NLP-7 neuropeptides signal to reduce egg laying both by inhibiting HSN and by activating $G\alpha_o$ in cells other than HSN. Thus, $G\alpha_o$ integrates diverse signals to maintain a bi-stable state of electrical excitability that dynamically controls circuit activity and behavior output in response to a changing environment.

.

bioRxiv preprint doi: https://doi.org/10.1101/701664; this version posted July 13, 2019. The copyright holder for this preprint (which was not certified by peer review) is the author/funder, who has granted bioRxiv a license to display the preprint in perpetuity. It is made available under aCC-BY 4.0 International license.

Introduction

A major goal of neuroscience is to understand how external and internal sensory signals control the activity of neural circuits to drive changes in animal behavior. Such sensory information triggers when a particular behavior should be initiated, for how long that behavior state should be continued, and under what conditions that behavior should be terminated. For example, hunger initiates searching behavior strategies to locate areas with food, and sensory feedback of local food availability triggers the termination of searching and the initiation of feeding (Flavell et al., 2013; Iwanir et al., 2016). Feeding behavior itself might terminate because external signals indicate food in the local area has been depleted, at which point searching strategies might resume (Lee et al., 2017; Scholz et al., 2017; Lopez-Cruz et al., 2019). Internal sensory feedback of satiety might also terminate both foraging and feeding in favor of other behaviors (You et al., 2008; Gallagher et al., 2013) like mating or reproduction (Gruninger et al., 2006; LeBoeuf et al., 2007; Gruninger et al., 2008). Extensive evidence has shown that neuromodulators like serotonin signal through presynaptic and postsynaptic G protein coupled receptors to drive these behavior state transitions (Jiang et al., 2001; Goulding et al., 2008). Yet, there is no neural circuit in any organism for which we know precisely how signaling events drive a serotonin-controlled behavior and how sensory input modulates these events. Small neural circuits typically found in invertebrate model organisms combine anatomical simplicity with uniquely powerful genetic and experimental accessibility, allowing for a complete understanding of the molecular basis for a behavioral output (Marder, 2012).

The *C. elegans* female reproductive circuit is ideally suited to study how environmental and internal sensory signals modulate decision making. The circuit is anatomically simple and drives alternative egg-laying behavior states that are characterized by ~20 minute inactive periods punctuated by ~2 minute active states in which ~4-6 eggs are laid in phase with the

bioRxiv preprint doi: https://doi.org/10.1101/701664; this version posted July 13, 2019. The copyright holder for this preprint (which was not certified by peer review) is the author/funder, who has granted bioRxiv a license to display the preprint in perpetuity. It is made available under aCC-BY 4.0 International license.

animal's locomotion (Waggoner et al., 1998; Collins and Koelle, 2013; Collins et al., 2016). As shown in Figure 1A, the circuit is comprised of two Hermaphrodite Specific Neurons (HSNs) that function as command neurons to promote the active state (Waggoner et al., 1998; Emtage et al., 2012). Three locomotion motor neurons (VA7, VB6, and VD7) and six cholinergic Ventral C neurons (VC1-6) synapse onto a set of egg-laying vulval muscles which contract to open the vulva to release eggs from the uterus into the environment (White et al., 1986). HSNs release serotonin and NLP-3 neuropeptides that signal to promote the active state of egg laying (Desai et al., 1988; Brewer et al., 2019). Serotonin signals through several distinct receptors expressed on vulval muscles (Carnell et al., 2005; Hobson et al., 2006; Xiao et al., 2006). *nlp-3* is predicated to encode multiple neuropeptides, suggesting multiple receptors may be required in discrete cells of the egg-laying circuit for NLP-3 activation of the egg-laying active state. Ca^{2+} imaging shows cells in the circuit have rhythmic, sequential activity as they enter active states characterized by 'bursts' of rhythmic Ca^{2+} activity that drive egg-laying events in phase with the body bends of locomotion (Zhang et al., 2008; Collins et al., 2016; Zang et al., 2017; Ravi et al., 2018a). HSN Ca^{2+} activity peaks ~2 seconds before each egg-laying vulval muscle Ca^{2+} transient within the active state, and optogenetic activation of the HSNs is sufficient to induce circuit activity and the active state (Collins et al., 2016). Animals bearing mutations that eliminate both serotonin and NLP-3 biosynthesis have reduced egg laying and show defects in vulval muscle Ca^{2+} activity (Brewer et al., 2019). However, despite strong delays in the onset of egg laying, HSN-deficient animals will eventually enter active states with coordinated vulval muscle Ca^{2+} activity that allows efficient egg release (Collins et al., 2016). These results indicate that while HSN activity is sufficient to induce circuit activity and behavior in adult animals, HSNs are not strictly required. Other signals must initiate the egg-laying active state in the absence of HSNs.

bioRxiv preprint doi: https://doi.org/10.1101/701664; this version posted July 13, 2019. The copyright holder for this preprint (which was not certified by peer review) is the author/funder, who has granted bioRxiv a license to display the preprint in perpetuity. It is made available under aCC-BY 4.0 International license.

We have recently identified a stretch-dependent homeostat that scales egg-laying circuit activity in response to feedback of egg accumulation. Juvenile and young adult animals lacking eggs in the uterus have low circuit activity, and optogenetic stimulation of the HSNs is unable to stimulate vulval muscle activity in these animals (Ravi et al., 2018a). Chemical or genetic sterilization leads to a reduction in both HSN and vulval muscle Ca^{2+} activity, locking animals in the inactive state (Collins et al., 2016; Ravi et al., 2018a). Acute chemogenetic silencing of vulval muscle electrical activity similarly blocks egg laying and presynaptic HSN Ca^{2+} activity. Reversal of this muscle silencing drives a homeostatic rebound in HSN 'burst' firing Ca^{2+} activity where 'bursts' of HSN Ca^{2+} transients promote ongoing circuit activity that drives release of the excess accumulated eggs (Ravi et al., 2018a). Feedback of successful egg release also signals to inhibit HSN activity. Four uv1 neuroendocrine cells which line the vulval canal are mechanically activated by the passage of eggs. The uv1 cells are peptidergic and tyraminergic, and inhibition of egg laying by tyramine requires the LGC-55 tyramine-gated Cl^- channel which is expressed on the HSNs (Collins et al., 2016). uv1 also expresses the FLP-11 and NLP-7 neuropeptides that signal to inhibit HSN activity and egg laying through receptors that remain unidentified (Banerjee et al., 2017). Full NLP-7 inhibition of egg laying requires the EGL-47 receptor and the G protein, $G\alpha_o$, both of which are expressed in HSN (Moresco and Koelle, 2004; Banerjee et al., 2017). HSN Ca^{2+} activity and egg laying are also inhibited by aversive signals from the external environment. Elevated environmental CO_2 activates BAG and other sensory neurons (Hallem et al., 2011; Fenk and de Bono, 2015). BAG releases FLP-17, which binds to EGL-6 receptors on HSN to activate $G\alpha_o$ to inhibit HSN activity, neurotransmitter release, and egg laying (Zang et al., 2017). A major open question is how competing, analog sensory inputs, from internal sensory feedback of sufficient egg accumulation promoting the active state, to external sensory information of an unfavorable environment, converge on the same neural circuit to drive unilateral, binary behavior decisions to enter or leave the egg-laying active state.

bioRxiv preprint doi: https://doi.org/10.1101/701664; this version posted July 13, 2019. The copyright holder for this preprint (which was not certified by peer review) is the author/funder, who has granted bioRxiv a license to display the preprint in perpetuity. It is made available under aCC-BY 4.0 International license.

The major G protein, $G\alpha_o$, mediates a large part of the modulatory signaling in the brain (Jiang et al., 2001), but our understanding of the biochemical consequences of $G\alpha_o$ signaling *in vivo* remain incomplete. Patient mutations in human *GNAO1* have been identified that disrupt $G\alpha_o$ plasma membrane localization and inhibition of voltage-gated Ca^{2+} currents in response to norepinephrine, with phenotypic consequences including epileptic encephalopathy (Nakamura et al., 2013). Discovering the conserved mechanisms by which $G\alpha_o$ inhibits synaptic transmission in simple neural circuits would inform the development of novel therapies for human disorders where $G\alpha_o$ has an important modulatory role. *C. elegans* $G\alpha_o$ shares more than 80% sequence identity with its corresponding mammalian ortholog, and knockout mutants show disrupted serotonin transmission along with hyperactive locomotion and egg-laying behaviors (Segalat et al., 1995; Koelle and Horvitz, 1996; Koelle, 2016). Loss of $G\alpha_o$ in *C. elegans* causes behavior phenotypes that precisely phenocopy the consequences of too much $G\alpha_q$ signaling through the PLCβ and Trio RhoGEF effector pathways (Brundage et al., 1996; Lackner et al., 1999; Miller et al., 1999; Williams et al., 2007). $G\alpha_o$ signaling is thought to modulate presynaptic ion channels (Qin et al., 1997; Peleg et al., 2002; Clancy et al., 2005; Mase et al., 2012), and genetic studies in *C. elegans* have identified the CCA-1 T-type voltage-gated Ca^{2+} channels, NCA Na^+ leak channels, and the IRK inward rectifying K^+ channels as potential downstream targets of $G\alpha_o$ signaling (Emtage et al., 2012; Topalidou et al., 2017a; Zang et al., 2017). How $G\alpha_o$ signaling itself affects egg-laying circuit activity and behavior has not been fully revealed. $G\alpha_o$ could signal within the active state to reduce the probability of HSN burst firing, shortening the duration of active states. Alternatively, $G\alpha_o$ may signal during the inactive state to reduce HSN excitability and the probability of entering the egg-laying active state. Whether and how such inhibitory signaling acts alongside the stretch-dependent homeostat is similarly unclear. $G\alpha_o$ signaling in HSN has been found to inhibit *tph-1* gene expression and serotonin biosynthesis

bioRxiv preprint doi: https://doi.org/10.1101/701664; this version posted July 13, 2019. The copyright holder for this preprint (which was not certified by peer review) is the author/funder, who has granted bioRxiv a license to display the preprint in perpetuity. It is made available under aCC-BY 4.0 International license.

(Tanis et al., 2008), suggesting long-term changes in serotonin transmission might also contribute to the dramatic egg-laying behavior phenotypes seen in $G\alpha_o$ signaling mutants.

Here we explore how $G\alpha_o$ signals to inhibit *C. elegans* egg-laying circuit activity and behavior. Our data reveal that $G\alpha_o$ signaling reduces the electrical excitability of a command neuron, allowing the circuit to execute a binary behavior decision upon the alignment of optimal external and internal sensory conditions.

Results

$G\alpha_o$ signaling inhibits egg-laying behavior in *C. elegans*. Animals with too much $G\alpha_o$ signaling retain eggs in their uterus, while $G\alpha_o$ loss-of-function or null mutants retain fewer eggs (Tanis et al., 2008). Embryos in such hyperactive egg-laying mutants also spend less time developing in the uterus and are laid at earlier stages of development, typically fewer than eight cells per embryo. Whether $G\alpha_o$ manipulations caused a change in the duration of the active state (e.g. how frequently eggs are laid within an active state), duration of the inactive state (how frequently animals enter an egg-laying active state), or both, remains unclear. To better understand how inhibitory $G\alpha_o$ signaling contributes to the pattern of circuit activity that underlies two-state behaviors, we analyzed the temporal pattern of egg laying during adult active states in $G\alpha_o$ signaling mutants.

Reduced inhibitory $G\alpha_o$ signaling leads to premature egg laying and decreases the duration of egg-laying inactive states

bioRxiv preprint doi: https://doi.org/10.1101/701664; this version posted July 13, 2019. The copyright holder for this preprint (which was not certified by peer review) is the author/funder, who has granted bioRxiv a license to display the preprint in perpetuity. It is made available under aCC-BY 4.0 International license.

We find that $G\alpha_o$ signals to inhibit the onset of egg laying. We performed a 'time to first egg' assay in wild-type animals and in mutants with too much or too little $G\alpha_o$ signaling. As previously described, wild-type animals release their first embryo ~6-7 hours after becoming adults (Ravi et al., 2018a). Animals bearing $G\alpha_o$ loss-of-function or null mutations laid their eggs much earlier, 3-4 hours after becoming adults (Figure 1B). *n1134*, a hypomorphic mutant predicted to lack the conserved N-terminal myristoylation and palmitoylation sequence, and *sa734*, an early stop mutant predicted to be a molecular null (Segalat et al., 1995; Robatzek and Thomas, 2000), showed a similar precocious onset in egg laying (Figure 1B). This phenotype was shared in transgenic animals where $G\alpha_o$ function was inhibited just in HSNs through the cell-specific expression of Pertussis Toxin (Tanis et al., 2008). Because the timing of this first egg-laying event requires serotonin and HSN activity (Ravi et al., 2018a), these results suggest that $G\alpha_o$ normally signals in HSN to inhibit neurotransmitter release and thereby delay the first egg-laying active state (Figure 1B). To test the effects of increased $G\alpha_o$ signaling, we analyzed the behavior of *egl-10(md176)* mutants which lack the major RGS protein that terminates $G\alpha_o$ signaling by promoting $G\alpha_o$ GTP hydrolysis (Koelle and Horvitz, 1996). *egl-10(md176)* mutants showed a strong and significant delay in the onset of egg laying, laying their first egg ~15 hours after reaching adulthood (Figure 1B); this delay is similar to animals without HSNs (Ravi et al., 2018a). This delay in egg laying phenotype was shared in transgenic animals expressing the constitutively active $G\alpha_o$ (Q205L) mutant specifically in the HSNs, consistent with $G\alpha_o$ signaling in HSN acting to inhibit neurotransmitter release.

To understand how $G\alpha_o$ signaling controls the normal two-state pattern of egg laying, we made long-term recordings of adults as they transitioned into and out of the active states in which clusters of several eggs are typically laid. Intervals between egg-laying events were operationally classified into two categories: intra-cluster intervals and inter-cluster intervals, as previously

bioRxiv preprint doi: https://doi.org/10.1101/701664; this version posted July 13, 2019. The copyright holder for this preprint (which was not certified by peer review) is the author/funder, who has granted bioRxiv a license to display the preprint in perpetuity. It is made available under aCC-BY 4.0 International license.

described (Waggoner et al., 1998; Collins and Koelle, 2013; Banerjee et al., 2017; Zang et al., 2017; Chew et al., 2018). Intra-cluster intervals (< 4 minutes) are intervals between consecutive egg laying events within a single active state. Inter-cluster intervals (> 4 minutes) are the intervals between distinct active states, and thus provide us with a measure of the frequency of egg-laying active states (Waggoner et al., 1998). Wild-type animals displayed a two-state pattern of egg laying with multiple egg-laying events clustered within brief, ~2 minute active states about every 20-30 minutes (Figure 1C and Table 1). Animals with reduced inhibitory $G\alpha_o$ signaling entered active states 2-3-fold more frequently, often laying single eggs during active states separated by only ~12-13 minutes (Figure 1C and Table 1). The pattern of egg-laying events in animals expressing Pertussis Toxin in the HSN neurons was indistinguishable from the *goa-1(n1134)* hyperactive egg laying mutant, indicating that $G\alpha_o$ signals in HSN to reduce the probability of entering the active state (Figure 1C; Figure Supplement 1; and Table 1). Loss of inhibitory $G\alpha_o$ signaling led to active states in which the 1-2 embryos in the uterus were laid almost immediately after they were positioned next to the vulval opening. As a result, successive egg-laying events were rate-limited by egg production, and the average intra-cluster intervals were typically double that of wild-type animals (Figure 1C, Figure Supplement 1, and Table 1). In contrast, *egl-10(md176)* mutant animals and animals expressing the $G\alpha_o$(Q205L) gain-of-function mutant in the HSNs had infrequent egg laying, lengthening the average inactive period to 258 and 67 min, respectively (Figure 1C, Supplemental Figure 1, and Table 1). Interestingly, animals with too much $G\alpha_o$ signaling still laid eggs in clusters of multiple eggs (Table 1), consistent with our results showing that a stretch-dependent homeostat can maintain the active state even when neurotransmitter release from the HSN is inhibited (Collins et al., 2016; Ravi et al., 2018a). These results show that $G\alpha_o$ signaling does not modulate patterns of egg laying within active states. Instead, $G\alpha_o$ specifically acts to determine how frequently animals enter into

bioRxiv preprint doi: https://doi.org/10.1101/701664; this version posted July 13, 2019. The copyright holder for this preprint (which was not certified by peer review) is the author/funder, who has granted bioRxiv a license to display the preprint in perpetuity. It is made available under aCC-BY 4.0 International license.

the egg-laying active state. In addition, these results suggest that $G\alpha_o$ signals to inhibit egg-laying behavior even under 'optimal' laboratory growth and culture conditions.

$G\alpha_o$ signaling inhibits HSN Ca^{2+} activity to promote the inactive behavior state

To understand how $G\alpha_o$ signaling regulates HSN activity, we performed ratiometric Ca^{2+} imaging in our panel of $G\alpha_o$ signaling mutants. Animals bearing the *goa-1(n1134)* hypomorphic or *goa-1(sa734)* null mutations that reduce inhibitory $G\alpha_o$ signaling showed a clear change in HSN Ca^{2+} activity from burst to more tonic firing (Figure 2A, Videos 1-3). Complete loss of inhibitory $G\alpha_o$ signaling caused a significant increase in the frequency of HSN Ca^{2+} transients (Figure 2B and 2C). We were surprised that the *goa-1(n1134)* mutants, which show strongly hyperactive egg-laying behavior indistinguishable from that of *goa-1(sa734)* null mutants, showed only a modest and insignificant increase in HSN Ca^{2+} activity compared to wild-type (Figure 2C). The *goa-1(n1134)* hypomorphic mutant is expected to have residual $G\alpha_o$ signaling activity in that its major defect is the absence of a proper membrane anchor sequence (Mumby et al., 1990). These results suggest that the hyperactive egg-laying phenotypes observed in *goa-1(n1134)* mutants are separable from changes in presynaptic HSN Ca^{2+} activity. Instead, these behavioral effects may be a consequence of inhibitory $G\alpha_o$ signaling outside of HSN and/or secondary changes in serotonin biosynthesis (Segalat et al., 1995; Tanis et al., 2008).

We next tested how increased inhibitory $G\alpha_o$ signaling affects HSN activity. Both *egl-10(md176)* mutants and transgenic animals expressing the activated GOA-1(Q205L) in HSNs showed a significant and dramatic reduction in the frequency of HSN Ca^{2+} transients, with single HSN Ca^{2+} transients occuring several minutes apart (Figure 2A and 2B). The rare egg-laying events seen in animals with increased $G\alpha_o$ signaling were mostly associated with single HSN Ca^{2+} transients, not the multi-transient bursts seen in wild-type animals (Figure 2A and 2C). In

bioRxiv preprint doi: https://doi.org/10.1101/701664; this version posted July 13, 2019. The copyright holder for this preprint (which was not certified by peer review) is the author/funder, who has granted bioRxiv a license to display the preprint in perpetuity. It is made available under aCC-BY 4.0 International license.

one *egl-10(md176)* animal, we observed one egg-laying event that was not accompanied by an HSN Ca^{2+} transient. This suggests that elevated $G\alpha_o$ signaling may effectively silence the HSNs, and that, in this case, egg laying becomes HSN-independent. Consistent with this model, complete silencing of HSNs in *egl-10(md176)* and *egl-1(n986dm)* mutants that lack HSNs show similar defects in the timing of first egg laid (Ravi et al., 2018a). Alternatively (or additionally) $G\alpha_o$ signaling may function to depress coordinated activity between the gap-junctioned, contralateral HSNs, whose Ca^{2+} activity we were unable to observe simultaneously because our confocal imaging conditions only captures one HSN at a time.

To determine how disruption of inhibitory $G\alpha_o$ signaling in HSN affects neuronal activity, we recorded HSN Ca^{2+} transients in transgenic animals expressing Pertussis Toxin specifically in the HSNs. $G\alpha_o$ silenced HSNs showed a dramatic increase in the frequency of HSN Ca^{2+} activity, leading to a nearly constitutive tonic firing activity similar to that observed in *goa-1(sa734)* null mutants (Figure 3A, 3B, and 3C; compare Videos 4 and 5). While control animals showed an average HSN Ca^{2+} transient frequency of about ~0.4 transients per minute, animals expressing Pertussis Toxin in HSN showed an average 1.9 transients per minute, a significant increase (Figure 3C). These results suggest that unidentified neurotransmitters and/or neuropeptides signal even under 'optimal' steady-state growth conditions to activate HSN receptors and $G\alpha_o$, to reduce cell excitability, allowing the observed two-state pattern of HSN activity and egg-laying behavior. Importantly, these results show that $G\alpha_o$ signals cell-autonomously in HSN to inhibit Ca^{2+} activity. Such changes in cell excitability by $G\alpha_o$ signaling are expected to precede presynaptic UNC-13 localization (Nurrish et al., 1999) and/or long-term changes in serotonin biosynthesis (Tanis et al. 2008).

We have previously shown that burst Ca^{2+} activity in the command HSN neurons is initiated and sustained by a stretch-dependent homeostat. In chemically or genetically sterilized

bioRxiv preprint doi: https://doi.org/10.1101/701664; this version posted July 13, 2019. The copyright holder for this preprint (which was not certified by peer review) is the author/funder, who has granted bioRxiv a license to display the preprint in perpetuity. It is made available under aCC-BY 4.0 International license.

animals, burst Ca^{2+} activity in HSN is largely eliminated (Ravi et al., 2018a). As such, we were surprised to observe high frequency Ca^{2+} transients in $G\alpha_o$ signaling mutants because these animals typically retain few (1 to 3) eggs in the uterus at steady state, conditions that normally eliminate HSN burst firing. We hypothesized that the stretch-dependent homeostat was not required to promote HSN Ca^{2+} activity in $G\alpha_o$ signaling mutants. To test this, we chemically sterilized transgenic animals expressing Pertussis Toxin in the HSNs with Floxuridine (FUDR), a blocker of embryogenesis, and recorded HSN Ca^{2+} activity. Wild-type animals treated with FUDR showed a dramatic decrease in the frequency of HSN Ca^{2+} activity and an elimination of burst firing (Figures 3A-C). Sterilized transgenic animals expressing Pertussis Toxin in the HSNs showed only a slight reduction in HSN Ca^{2+} frequency (Figure 3A and 3B). Both fertile and sterile Pertussis Toxin expressing animals had significantly increased HSN Ca^{2+} transient frequency (~1.9 / min), indicating their HSNs no longer require the retrograde signals of egg accumulation arising from the stretch-homeostat. One explanation for this could be that in wild-type animals, the retrograde burst-inducing signal is necessary to maintain firing threshold in the presence of inhibitory $G\alpha_o$ signaling.

Presynaptic $G\alpha_o$ signaling inhibits postsynaptic vulval muscle activity

To test how changes in inhibitory $G\alpha_o$ signaling affect the postsynaptic vulval muscles, we recorded Ca^{2+} activity in the vulval muscles of *goa-1(n1134)* mutant and Pertussis Toxin expressing transgenic animals. Active states were operationally defined as beginning one minute before the laying of the first egg and concluding one minute after the last egg-laying event. As shown in Figure 4, inactive state vulval muscle Ca^{2+} twitching activity is slightly increased in *goa-1(n1134)* mutants but is dramatically increased in transgenic animals expressing Pertussis

bioRxiv preprint doi: https://doi.org/10.1101/701664; this version posted July 13, 2019. The copyright holder for this preprint (which was not certified by peer review) is the author/funder, who has granted bioRxiv a license to display the preprint in perpetuity. It is made available under aCC-BY 4.0 International license.

Toxin in the presynaptic HSN neurons, confirming an increase in neurotransmitter release from the HSNs. Surprisingly, egg-laying active state Ca^{2+} activity in *goa-1(n1134)* mutants was not significantly different from that seen in wild-type control animals (Figure 4A and 4B; compare Videos 6 and 7). In contrast, the frequency of strong vulval muscle Ca^{2+} transients that accompany the active states was significantly increased in animals expressing Pertussis Toxin in HSN (Figure 4C and 4D; compare Videos 8 and 9). We have previously shown that egg accumulation promotes vulval muscle excitability during the active state while sterilization reduces vulval muscle activity to that of the inactive state (Collins et al., 2016; Ravi et al., 2018a). To our surprise, FUDR treatment significantly reduced vulval muscle Ca^{2+} activity in animals expressing Pertussis Toxin in HSN (Figure 4C and 4D), despite the FUDR-insensitivity of presynaptic HSN Ca^{2+} activity in these animals (Figure 3C). Vulval muscle Ca^{2+} activity after FUDR treatment was still higher in animals expressing Pertussis Toxin in HSNs compared to similarly treated wild-type animals (Figure 4C and 4D). This result suggests that vulval muscle activity remains dependent on egg accumulation and/or germline activity even when HSN activity is dramatically increased. However, because these animals lay eggs almost as soon as they are made, the degree of stretch necessary to induce the active state must be markedly reduced.

$G\alpha_o$ signaling modulates the HSN resting membrane potential

Reduction of inhibitory $G\alpha_o$ signaling strongly increased HSN Ca^{2+} activity and burst firing, prompting us to investigate whether $G\alpha_o$ signaling modulates HSN electrical excitability. We recorded the resting membrane potential of the HSN neurons in animals with altered $G\alpha_o$ signaling using the whole-cell patch clamp method (Figure 5A), as described (Yue et al., 2018). Hypomorphic *goa-1(n1143)* loss-of-function mutants displayed a trend towards more

bioRxiv preprint doi: https://doi.org/10.1101/701664; this version posted July 13, 2019. The copyright holder for this preprint (which was not certified by peer review) is the author/funder, who has granted bioRxiv a license to display the preprint in perpetuity. It is made available under aCC-BY 4.0 International license.

depolarized resting potentials (-17.9 mV) compared to wild-type animals (-21.1 mV), but this difference was not statistically significant (Figure 5B). In contrast, the resting membrane potential of HSNs in *egl-10(md176)* $G\alpha_o$ RGS protein mutant animals with a global increase in $G\alpha_o$ signaling (Koelle and Horvitz, 1996) was significantly hyperpolarized (-40.8 mV) compared to wild-type control animals. This hyperpolarization of HSNs in *egl-10(md176)* mutants explains the reduced frequency of HSN Ca^{2+} transients and their strongly reduced egg-laying behavior. Transgenic animals expressing Pertussis Toxin specifically in the HSNs had significantly depolarized HSNs (-14.75 mV) compared to the wild-type parental strain (-21.8 mV). These results show that $G\alpha_o$ signals in the HSNs to promote membrane polarization, reducing cell Ca^{2+} activity and neurotransmitter release.

Inhibition of egg laying by $G\alpha_o$ is not replicated by elevated βγ expression

Receptor activation of $G\alpha_{i/o}$ heterotrimers releases βγ subunits which have previously been shown to bind to activate specific K^+ channels and inhibit Ca^{2+} channels (Reuveny et al., 1994; Herlitze et al., 1996). To test if over-expression of βγ subunit in HSN would similarly inhibit egg laying, we transgenically overexpressed the *C. elegans* Gβ protein and Gγ protein subunits GPB-1 and GPC-2 under the *tph-1* promoter along with GFP. We did not observe any significant differences in steady-state egg accumulation Figure 5C. The number of eggs stored *in-utero* in these animals (13.0±1.1) was comparable to wildtype animals (15.7±1.2) and less than *egl-10(md176)* mutant animals (44.53±2.3). These results suggest that $G\alpha_o$ signals to inhibit HSN activity and egg laying via effectors distinct from simple titration or release of βγ subunits.

Egg-laying behavior is dysregulated in cAMP and cGMP signaling mutants

bioRxiv preprint doi: https://doi.org/10.1101/701664; this version posted July 13, 2019. The copyright holder for this preprint (which was not certified by peer review) is the author/funder, who has granted bioRxiv a license to display the preprint in perpetuity. It is made available under aCC-BY 4.0 International license.

As shown in Figure 5D (top) receptor activation of $G\alpha_{i/o}$ heterotrimers may also affect cAMP or cGMP levels and their subsequent activation of protein kinases (Kobayashi et al., 1990; Zhang and Pratt, 1996; Matsubara, 2002; Ghil et al., 2006). Receptor activation of $G\alpha_s$ activates adenylate cyclase, and the cAMP produced activates protein kinase A (PKA) which phosphorylates unidentified downstream effectors to augment neurotransmitter release (Koelle, 2016). Mutations that increase $G\alpha_s$ signaling in *C. elegans* cause hyperactive locomotion resembling that of animals lacking inhibitory $G\alpha_o$ signaling (Schade et al., 2005; Charlie et al., 2006a). How $G\alpha_s$ and cAMP signaling affect egg-laying behavior and whether this is antagonized by $G\alpha_o$ has not been previously reported. We find that animals carrying *gsa-1(ce81)* gain-of-function mutations predicted to increase $G\alpha_s$ signaling accumulate fewer eggs compared to wild-type animals (Figure 5D, middle). Because a reduction in steady-state egg accumulation could result from indirect effects on egg production or brood size, we examined the developmental age of embryos laid. Loss of inhibitory $G\alpha_o$ signaling causes embryos to be laid previously, before they reach the 8-cell stage (Figure 5D, bottom). $G\alpha_s$ gain-of-function mutant animals do not show a corresponding increase in early-stage embryos that are laid, suggesting the reduction in egg accumulation observed is indirect. In contrast, gain-of-function *acy-1* Adenylate Cyclase mutations or loss-of-function *pde-4* phosphodiesterase mutations, both predicted to increase cAMP signaling (Schade et al., 2005; Charlie et al., 2006a), cause animals to accumulate fewer eggs and lay them at earlier stages (Figure 5D). Similarly, *kin-2* mutant animals predicted to have increased Protein Kinase A activity (Schade et al., 2005) showed a modest but significant hyperactive egg-laying phenotype. Together, these results indicate that $G\alpha_s$, cAMP, and Protein Kinase A signal to promote egg-laying behavior, phenotypes which are consistent with $G\alpha_o$ acting to antagonize $G\alpha_s$ signaling.

bioRxiv preprint doi: https://doi.org/10.1101/701664; this version posted July 13, 2019. The copyright holder for this preprint (which was not certified by peer review) is the author/funder, who has granted bioRxiv a license to display the preprint in perpetuity. It is made available under aCC-BY 4.0 International license.

Previous work has shown that loss of the cGMP-dependent Protein Kinase G in *C. elegans* reduces egg laying (Trent et al., 1983; Fujiwara et al., 2002; L'Etoile et al., 2002; Raizen et al., 2006; Hao et al., 2011). Mutations which increase activity of Protein Kinase G increase egg laying while loss of Protein Kinase G signaling reduces it (Figure 5D, middle). To determine whether $G\alpha_o$ and Protein Kinase G regulate egg laying in a shared pathway, we performed a genetic epistasis experiment. *goa-1(sa734)*; *egl-4(n479)* double null mutants accumulate very few eggs (Figure 5D, middle), resembling the *goa-1(sa734)* null mutant. However, the low brood size of the *goa-1(sa734)* mutant could prevent accurate measurement of these animal's egg-laying defects. To address this, we measured the stage of eggs laid. Loss of the EGL-4 Protein Kinase G strongly and significantly suppressed the hyperactive egg-laying behavior of $G\alpha_o$ null mutants (Figure 5D, bottom). *goa-1(sa734)*; *egl-4(n479)* mutants laid 33% of their embryos at early stages compared to 88% for the *goa-1(sa734)* single mutant. The eggs laid by these double mutants were at wild-type stages of development, not at late stages typically observed from *egl-4(n479)* single mutants (Trent et al., 1983). These results are consistent with $G\alpha_o$ acting upstream or parallel to cGMP and/or Protein Kinase G signaling to regulate egg-laying behavior.

$G\alpha_o$ signals in other cells of the egg-laying circuit to regulate behavior

GOA-1 is expressed in all neurons of the reproductive circuit, the egg-laying vulval muscles, and the uv1 neuroendocrine cells (Jose et al., 2007), raising questions as to what $G\alpha_o$ is doing in those cells to regulate egg-laying behavior. Previous work has shown that transgenic expression of the activated GOA-1(Q205L) specifically in the HSNs, and not the VCs or vulval muscles, was sufficient to rescue the hyperactive egg-laying behavior of *goa-1(n1134)* mutants (Tanis et al., 2008). Previous work failing to identify a function for $G\alpha_o$ in the vulval muscles used

bioRxiv preprint doi: https://doi.org/10.1101/701664; this version posted July 13, 2019. The copyright holder for this preprint (which was not certified by peer review) is the author/funder, who has granted bioRxiv a license to display the preprint in perpetuity. It is made available under aCC-BY 4.0 International license.

a modified *Nde*-box element from the *ceh-24* promoter that drives expression more efficiently in the vm1 muscle cells compared to the vm2 muscles innervated by the HSN and VC neurons. Expression of Pertussis Toxin in both vm1 and vm2 vulval muscles from a larger region of the *ceh-24* gene promoter (Harfe and Fire, 1998; Ravi et al., 2018a), failed to cause any significant changes in the steady-state egg accumulation (Figure 5–figure supplement 1A). Conversely, expression of the activated GOA-1(Q205L) in the vulval muscles form the same promoter did cause a modest but significant egg-laying defect, with animals accumulating 24.1±2.0 eggs compared to mCherry-expressing control animals (13.2±0.7 eggs). This egg-laying defect was significantly weaker than *egl-10(md176)* mutants or transgenic animals expressing GOA-1(Q205L) in the HSNs. We do not believe this modest egg-laying defect was caused by transgene expression outside of the vulval muscles, as expression of Tetanus Toxin from the *ceh-24* promoter showed no such egg-laying defect (Figure 5–figure supplement 1B). Collectively, these results show that $G\alpha_o$ does not play a significant role in suppressing vulval muscle excitability under state-state conditions but activated $G\alpha_o$ can signal in these cells to induce a mild but significant inhibition of cell activity and egg-laying behavior.

The uv1 cells synthesize and release neurotransmitter tyramine and neuropeptides encoded by genes *nlp-7* and *flp-11* which inhibit egg laying (Alkema et al., 2005; Collins et al., 2016; Banerjee et al., 2017). Based on the function of $G\alpha_o$ signaling in inhibiting neurotransmitter release in neurons, we would expect that loss of $G\alpha_o$ in uv1 would enhance excitability, promoting release of inhibitory tyramine and neuropeptides, causing a reduction of egg laying. Surprisingly, previous work has shown that transgenic expression of Pertussis Toxin in uv1 cells increased the frequency of early-stage eggs that are laid, similar to the blocking of neurotransmitter release by Tetanus Toxin (Jose et al., 2007). A caveat of these experiments was that transgene expression was driven by the *ocr-2* gene promoter that, in addition to the

bioRxiv preprint doi: https://doi.org/10.1101/701664; this version posted July 13, 2019. The copyright holder for this preprint (which was not certified by peer review) is the author/funder, who has granted bioRxiv a license to display the preprint in perpetuity. It is made available under aCC-BY 4.0 International license.

uv1 cells, is also expressed in the utse (uterine-seam) associated cells and head sensory neurons. To test whether $G\alpha_o$ functions specifically in uv1 to regulate egg laying we used the *tdc-1* gene promoter (Alkema et al., 2005) along with the *ocr-2* 3' untranslated region (Jose et al., 2007) to drive expression more specifically in uv1. Expression of Pertussis Toxin in uv1 caused a significant decrease in steady-state egg accumulation (10.9±1.5) compared to mCherry-expressing control animals (15.3±1.2) (Figure 5–figure supplement 1C). We also tested how elevated $G\alpha_o$ signaling in uv1 affects egg laying. Transgenic expression of the activated GOA-1(Q205L) mutant in uv1 cells caused no quantitative differences in egg accumulation (15.5±2.1 eggs) (Figure 5–figure supplement 1C). Together, these results show that $G\alpha_o$ has a limited role in regulating egg-laying behavior in the vulval muscles or uv1 neuroendocrine cells, unlike the strong phenotypes observed when we manipulate $G\alpha_o$ function in HSN.

Neuropeptide NLP-7 signals through $G\alpha_o$ to inhibit egg laying independent of the HSNs

Multiple neuropeptides and receptors have been identified that are thought to inhibit egg laying via signaling through $G\alpha_o$-coupled receptors expressed on HSN (Figure 1A). FLP-17 and FLP-10 neuropeptides activate the $G\alpha_o$-coupled EGL-6 receptors on the HSN to inhibit egg laying, and this inhibition depends upon the IRK-1 K^+ channel which functions to depress HSN excitability (Ringstad and Horvitz, 2008; Emtage et al., 2012). Gain-of-function mutations in the HSN-expressed gustatory-like receptor, EGL-47, also strongly inhibit egg-laying behavior (Moresco and Koelle, 2004). Genetic epistasis experiments are consistent with the interpretation that EGL-47, like EGL-6, signals through $G\alpha_o$ in the HSNs to inhibit egg laying, but the ligands which activate EGL-47 are not known (Moresco and Koelle, 2004). Recent work has identified NLP-7 neuropeptides, synthesized in the VC neurons and uv1 neuroendocrine cells, as potential

bioRxiv preprint doi: https://doi.org/10.1101/701664; this version posted July 13, 2019. The copyright holder for this preprint (which was not certified by peer review) is the author/funder, who has granted bioRxiv a license to display the preprint in perpetuity. It is made available under aCC-BY 4.0 International license.

ligands for EGL-47 and $G\alpha_o$ signaling (Banerjee et al., 2017). Animals overexpressing the NLP-7 neuropeptide are highly egg-laying defective, accumulating 39.6±3.4 eggs in the uterus (Figure 6A). To test how NLP-7 signals through $G\alpha_o$ to inhibit HSN activity and egg laying, we crossed NLP-7 over-expressing transgenes into *goa-1* mutant animals and evaluated their egg-laying behavior phenotypes. *goa-1(n1134)* loss-of-function and *goa-1(sa734)* null mutants showed a mild and strong suppression of the egg-laying defect of NLP-7 overexpressing animals with animals storing 23.3±2.5 and 9.3±1.8 eggs, respectively (Figure 6A). To confirm that $G\alpha_o$ was required for NLP-7 inhibition of egg laying, we measured the stage of embryos laid by these animals. *goa-1(sa734)* null mutant animals over-expressing NLP-7 laid ~100% of their embryos at early stages, and this was not significantly different from 98% of embryos laid at early stages by *goa-1(sa734)* single mutant animals (Figure 6B). Together, these results strongly suggest that NLP-7 neuropeptides signal to activate $G\alpha_o$ and inhibit egg laying.

Since the HSNs appear to be the principal sites of inhibitory $G\alpha_o$ signaling, we tested how NLP-7 over-expression affects HSN Ca^{2+} activity. As expected, over-expression of NLP-7 strongly inhibited HSN Ca^{2+} activity (Figure 6C and 6D), consistent with the strong egg-laying defects of these animals. To our surprise, loss of $G\alpha_o$ failed to restore HSN Ca^{2+} transient activity in NLP-7 overexpressing animals, despite showing the strong hyperactive egg-laying behavior of *goa-1(sa734)* single mutants. These results indicate that although NLP-7 signals to silence HSN Ca^{2+} activity, it does not require $G\alpha_o$ function to do so. Moreover, it suggests that egg laying in animals fully lacking inhibitory $G\alpha_o$ signaling is independent of HSN activity, consistent with previous results that report *goa-1* null mutants lacking HSNs still lay primarily early-stage eggs (Segalat et al., 1995). Thus, NLP-7 neuropeptides and $G\alpha_o$ signal to inhibit egg-laying behavior through cellular targets other than the HSNs.

bioRxiv preprint doi: https://doi.org/10.1101/701664; this version posted July 13, 2019. The copyright holder for this preprint (which was not certified by peer review) is the author/funder, who has granted bioRxiv a license to display the preprint in perpetuity. It is made available under aCC-BY 4.0 International license.

Discussion

Using a combination of genetic, imaging, physiological, and behavioral approaches, we found that the conserved G protein, $G\alpha_o$, coordinates behavior transitions between periods of embryo accumulation and release. Activated $G\alpha_o$ signals to depress HSN command neuron excitability and neurotransmitter release, ensuring the egg-laying circuit becomes active only when sufficient eggs in the uterus. Without inhibitory $G\alpha_o$ signaling, presynaptic HSN command neurons remain excitable, and HSN Ca^{2+} activity becomes tonic and insensitive to retrograde feedback from the stretch-dependent homeostat. As a result, animals lacking $G\alpha_o$ enter the egg-laying active state twice as frequently as wild-type animals. In spite of this, the hyperactive egg-laying behavior of $G\alpha_o$ mutant animals is not 'constitutive.' The increased postsynaptic vulval muscle Ca^{2+} activity of $G\alpha_o$ mutants requires egg accumulation and remains sensitive to sterilization, suggesting that feedback of egg accumulation acts primarily on the vulval muscles. Conversely, the HSNs are hyperpolarized in animals with too much inhibitory $G\alpha_o$ signaling, and behavior and pharmacological experiments suggest they rarely release neurotransmitters (Trent et al., 1983; Koelle and Horvitz, 1996). As a result, the timing of egg-laying active states in animals with elevated inhibitory $G\alpha_o$ signaling appears largely driven by an increase in activity in cells other than HSN.

Our results inform our understanding of how G protein signaling modulates the stretch-dependent homeostat that governs egg-laying behavior (Figure 7). Egg laying in wild-type animals typically begins ~6 hours after the L4-adult molt upon the accumulation of 5-8 eggs in the uterus (Ravi et al., 2018a). Loss of inhibitory $G\alpha_o$ signaling causes the first egg-laying event to occur ~2 hours earlier, with one or two embryos being laid soon after they are deposited into the uterus. Conversely, mutations that increase inhibitory $G\alpha_o$ signaling delay egg laying to a

bioRxiv preprint doi: https://doi.org/10.1101/701664; this version posted July 13, 2019. The copyright holder for this preprint (which was not certified by peer review) is the author/funder, who has granted bioRxiv a license to display the preprint in perpetuity. It is made available under aCC-BY 4.0 International license.

similar extent as loss of HSNs, until feedback of egg accumulation is sufficient to drive egg-laying circuit activity and behavior (Collins et al., 2016; Ravi et al., 2018a). Mutations in the excitatory $G\alpha_q$ signaling pathway show precisely the opposite phenotypes as those seen for $G\alpha_o$, with eggs being laid later when $G\alpha_q$ signaling is reduced and earlier when $G\alpha_q$ signaling is increased (Bastiani et al., 2003). Aversive sensory input, or feedback of successful egg release, drives release of neurotransmitters and neuropeptides that signal through inhibitory receptors and $G\alpha_o$ to promote exit of the egg-laying active state. Together, these results suggest a working two-state model for how a balance of inhibitory and excitatory signaling through distinct G proteins is responsible for the accumulation of 12-15 eggs at steady-state and the laying of 3-5 eggs per active state (Figure 7).

Does G protein signaling control circuit excitability via modulation of the stretch-dependent homeostat? $G\alpha_o$ signaling directly affects HSN cell excitability, but in the absence of HSNs, animals still initiate egg laying after sufficient egg accumulation in the uterus, and this circuit activity is eliminated upon sterilization (Collins et al., 2016). Thus, even though modulation of HSN activity is a major consequence of the stretch-dependent homeostat, the homeostat still operates in the absence of HSN function. Consistent with this result, HSNs where $G\alpha_o$ function is blocked through cell-specific expression of Pertussis Toxin show little loss of Ca^{2+} activity after chemical sterilization. However, in these animals, vulval muscle Ca^{2+} activity is still significantly reduced by sterilization. This result suggests even dramatically potentiated HSN Ca^{2+} activity cannot drive egg-laying without feedback of egg accumulation. This stretch-dependent, homeostatic gating of HSN is consistent with our previous results showing that optogenetic stimulation of HSNs fails to induce vulval muscle Ca^{2+} activity in animals with too few eggs in the uterus (Ravi et al., 2018a). Despite the dramatic increase in vulval muscle Ca^{2+} transient frequency upon HSN-specific inactivation of $G\alpha_o$, we rarely observe strong egg-laying muscle

bioRxiv preprint doi: https://doi.org/10.1101/701664; this version posted July 13, 2019. The copyright holder for this preprint (which was not certified by peer review) is the author/funder, who has granted bioRxiv a license to display the preprint in perpetuity. It is made available under aCC-BY 4.0 International license.

contractions until there is an egg properly position above the vulva. This suggests the presence of conditional, feed-forward signaling mechanisms that provide additional excitatory input into the vulval muscles when an egg is ready for release. Determining whether the stretch-dependent homeostat modulates circuit activity via direct effects on cell electrical excitability, or through indirect signaling mechanisms, will require the identification of molecules and their sites of action within the stretch-dependent homeostat. We predict that loss of molecules required for detecting egg accumulation and uterine stretch would disrupt the observed rebound of egg-laying behavior after acute inhibition by aversive sensory signaling, starvation, or acute circuit silencing (Dong et al., 2000; Ravi et al., 2018a).

Our work suggests $G\alpha_o$ signals in HSN and in cells outside of the egg-laying circuit to inhibit egg-laying behavior. GOA-1 is expressed in all *C. elegans* neurons and muscle cells (Mendel et al., 1995; Segalat et al., 1995) along with cells in the egg-laying circuit (Jose et al., 2007). Pertussis Toxin expression in the HSNs causes hyperactive egg-laying behavior phenotypes that closely resemble *goa-1* null and loss-of-function mutants (Tanis et al., 2008). By contrast, Pertussis Toxin expression in VCs, vulval muscles, or uv1 causes no or very modest increase in egg laying (Tanis et al., 2008). Expression of the Q205L GTP-locked $G\alpha_o$ mutant in HSNs delays the onset of egg laying and steady-state egg accumulation to a similar degree as *egl-10* mutants lacking the $G\alpha_o$ RGS protein or animals without HSNs, leading to the suggestion that $G\alpha_o$ largely functions in HSN to inhibit neurotransmitter release and egg laying (Koelle and Horvitz, 1996; Tanis et al., 2008; Ravi et al., 2018a). However, *goa-1* null mutants lacking HSNs still show hyperactive egg-laying behavior (Segalat et al., 1995), suggesting that $G\alpha_o$ signals to inhibit neurotransmitter release in cells other than HSN to regulate egg laying. We find that NLP-7 over-expression largely silences HSN Ca^{2+} activity and blocks egg-laying behavior, consistent with previous results (Banerjee et al., 2017). Our data further show that NLP-7 inhibition of egg

bioRxiv preprint doi: https://doi.org/10.1101/701664; this version posted July 13, 2019. The copyright holder for this preprint (which was not certified by peer review) is the author/funder, who has granted bioRxiv a license to display the preprint in perpetuity. It is made available under aCC-BY 4.0 International license.

laying requires $G\alpha_o$ function, but that loss of $G\alpha_o$ does not rescue NLP-7 inhibition of HSN Ca^{2+} activity. This suggests that NLP-7 signals to inhibit HSN and egg laying via distinct pathways. NLP-7 is predicted to be processed into four distinct peptides, and previous work has shown that NLP-7 inhibition of egg laying requires EGL-47, a receptor expressed on HSN (Banerjee et al., 2017). Because EGL-47 inhibition of HSN activity and egg laying depends upon Cl^- extruding transporters KCC-2 and ABTS-1 (Tanis et al., 2009; Bellemer et al., 2011), different NLP-7 peptides may activate distinct receptors on HSN and other cells to inhibit egg laying. NLP-7 over-expression causes additional behavior phenotypes including sluggish locomotion, and $G\alpha_o$ signals to inhibit neurotransmitter release from cholinergic motor neurons that synapse onto the body wall muscles that drive locomotion. Our previous work has shown that the vulval muscles are rhythmically excited in phase with locomotion, and that this input into the vulval muscles is enhanced during the egg-laying active state (Collins and Koelle, 2013). We proposed that the VA7 and VB6 motor neurons that synapse onto the vm1 vulval muscles may mediate this rhythmic input into the vulval muscles (White et al., 1986; Collins et al., 2016). As such, NLP-7 may signal through $G\alpha_o$-coupled receptors on the VA/VB motor neurons to inhibit acetylcholine release. Global loss of $G\alpha_o$ inhibition may result in sufficiently high levels of ACh release from these motor neurons to hyperactivate vulval muscle Ca^{2+} activity and drive egg release.

Several models for how $G\alpha_o$ signals to regulate neurotransmitter release have been proposed, and our work is consistent with $G\alpha_o$ acting to inhibit multiple G protein effector pathways instead of within a single, dedicated pathway. A major target of $G\alpha_{i/o}$ family of G proteins include inward rectifying K^+ channels thought to be activated by release of $\beta\gamma$ subunits (Hille, 1994). Previous work has shown the IRK-1 K^+ channel is expressed in HSN and is required for inhibition of egg laying by the $G\alpha_o$-coupled EGL-6 neuropeptide receptor (Emtage et al., 2012). We do not observe behavior phenotypes upon over-expression of $\beta\gamma$ in HSN,

bioRxiv preprint doi: https://doi.org/10.1101/701664; this version posted July 13, 2019. The copyright holder for this preprint (which was not certified by peer review) is the author/funder, who has granted bioRxiv a license to display the preprint in perpetuity. It is made available under aCC-BY 4.0 International license.

suggesting $G\alpha_o$ may signal to inhibit HSN activity via direct effectors of the $G\alpha$ subunit. We find that mutations which increase cAMP and cGMP signaling cause hyperactive egg-laying behavior phenotypes that resemble loss of inhibitory $G\alpha_o$ signaling. Such phenotypes would be consistent with a model where $G\alpha_o$ signals to inhibit cAMP production and/or activate cGMP-specific phosphodiesterases. Protein Kinase G signaling has been shown to regulate the expression of a secreted protein in the uterine epithelium whose levels correlate with egg-laying rate (Hao et al., 2011). cAMP and cGMP signaling has well-established roles in the regulation of muscle contractility in response to stretch (Tsai and Kass, 2009). Because feedback of egg accumulation directly modulates egg-laying circuit activity, future work will be required to determine the relationship between $G\alpha_o$ signaling, cyclic nucleotides, and uterine stretch in the sensory modulation of the stretch-dependent homeostat.

Loss of inhibitory $G\alpha_o$ signaling converts HSN Ca^{2+} activity from two-state bursting to tonic firing. Genetic studies have identified several Na^+ and Ca^{2+} channels that regulate egg laying whose modulation by G protein signaling might underlie changes in HSN activity. NALCN Na^+ leak channels are expressed in HSN, and gain-of-function mutations increase HSN Ca^{2+} activity and cause hyperactive egg-laying behavior (Yeh et al., 2008). Genetically, NALCN channels are downstream of both $G\alpha_o$ and $G\alpha_q$, suggesting that NALCN channels could be targets for direct modulation by either or both G protein signaling pathways (Lutas et al., 2016; Topalidou et al., 2017b). Recent work has also shown that $G\alpha_q$ promotes neurotransmitter release via Ras/ERK/MAPK signaling (Coleman et al., 2018). Recent work has shown that TMC channels are similarly responsible for a background Na^+ leak conductance in both HSN and the vulval muscles that promotes cell excitability and egg-laying behavior (Yue et al., 2018). At present, genetic epistasis experiments have not determined whether TMC channels act in parallel to or downstream of G protein signaling. As such, $G\alpha_o$ and $G\alpha_q$ signaling may modulate egg-laying

bioRxiv preprint doi: https://doi.org/10.1101/701664; this version posted July 13, 2019. The copyright holder for this preprint (which was not certified by peer review) is the author/funder, who has granted bioRxiv a license to display the preprint in perpetuity. It is made available under aCC-BY 4.0 International license.

circuit activity via differential activation of protein kinases which phosphorylate TMC and/or NALCN channels to regulate their activity or surface expression. Modulation of voltage-gated Ca^{2+} channels might also contribute to the observed changes in HSN electrical excitability. HSN expresses L-type, P/Q-type, and T-type Ca^{2+} channels (Mathews et al., 2003; Zang et al., 2017), and mutations of these channels disrupt egg-laying behavior (Schafer and Kenyon, 1995; Lee et al., 1997; Mathews et al., 2003; Gao and Zhen, 2011; Laine et al., 2014). Mutations that increase Ca^{2+} channel opening at lower voltages cause hyperactive egg-laying behavior, consistent with these channels acting to promote depolarization of both the HSNs and vulval muscles. Recent studies have shown that both neurons and muscles in *C. elegans* show Ca^{2+} dependent spiking (Gao and Zhen, 2011; Liu et al., 2011; Liu et al., 2018), and these are regulated by both L-type (EGL-19) and T-type (CCA-1) Ca^{2+} channels. T-type channels such as CCA-1 can contribute to a 'window current' where the channel can pass current at depolarized potentials that are insufficient to trigger channel inactivation (Zang et al., 2017). Activation of these window currents might allow neurons like HSN to shift from spontaneous tonic firing to high frequency Ca^{2+} bursting. Future work leveraging the powerful molecular tools uniquely available in *C. elegans* and the egg-laying circuit along with direct physiological measurements should provide deep mechanistic insight into how medically important neuromodulators like serotonin and neuropeptides signal through $G\alpha_o$ and $G\alpha_q$ to shape patterns of circuit activity in health and human disease.

bioRxiv preprint doi: https://doi.org/10.1101/701664; this version posted July 13, 2019. The copyright holder for this preprint (which was not certified by peer review) is the author/funder, who has granted bioRxiv a license to display the preprint in perpetuity. It is made available under aCC-BY 4.0 International license.

Materials and Methods

Nematode Culture and Developmental Staging

Caenorhabditis elegans hermaphrodites were maintained at 20°C on Nematode Growth Medium (NGM) agar plates with *E. coli* OP50 as a source of food as described (Brenner, 1974). For assays involving young adults, animals were age-matched based on the timing of completion of the L4 larval molt. All assays involving adult animals were performed using age-matched adult hermaphrodites 20-40 hours past the late L4 stage. Table 2 lists all strains used in this study and their genotypes.

Plasmid and Strain Construction

Calcium reporter transgenes

HSN Ca^{2+}: HSN Ca^{2+} activity was visualized using LX2004 *vsIs183* [*nlp-3::GCaMP5::nlp-3 3'UTR + nlp-3::mCherry::nlp-3 3'UTR + lin-15(+)*] *lite-1(ce314) lin-15(n765ts) X* strain expressing GCaMP5G and mCherry from the *nlp-3* promoter as previously described (Collins et al., 2016). To visualize HSN Ca^{2+} activity in $G\alpha_o$ signaling mutants, we crossed LX2004 *vsIs183 lite-1(ce314) lin-15(n765ts) X* males with MT2426 *goa-1(n1134) I*, DG1856 *goa-1(sa734) I*, and MT8504 *egl-10(md176) V* hermaphrodites, and the fluorescent cross-progeny were allowed to self, generating MIA210 *goa-1(n1143) I*; *vsIs183 X lite-1(ce314) lin-15 (n765ts) X,* MIA263 *goa-1(sa734) I*; *vsIs183 X lite-1(ce314) lin-15 (n765ts) X*, and MIA216 *egl-10(md176) V; vsIs183 lite-1(ce314) lin-15(n765ts) X* strains, respectively. We noticed repulsion between *vsIs183* and the *vsIs50* transgene that expresses the catalytic subunit of Pertussis Toxin from the *tph-1* promoter, suggesting both were linked to the X chromosome. As such, LX850 *vsIs50 lin-15(n765ts) X* males were crossed with LX1832 *lite-1(ce314) lin-15(n765ts) X* hermaphrodites, the non-Muv

bioRxiv preprint doi: https://doi.org/10.1101/701664; this version posted July 13, 2019. The copyright holder for this preprint (which was not certified by peer review) is the author/funder, who has granted bioRxiv a license to display the preprint in perpetuity. It is made available under aCC-BY 4.0 International license.

progeny were allowed to self, and homozygous *lite-1(ce314)* non-Muv animals were kept, generating the strain MIA218 *vsIs50 lite-1(ce314) lin-15(n765ts) X.* MIA218 males were then crossed with LX2007 *vsIs186; lite-1(ce314) lin-15(n765ts) X*; the cross-progeny were allowed to self, generating MIA227 *vsIs186; vsIs50 lite-1(ce314) lin-15(n765ts) X*. In order to visualize HSN Ca^{2+} activity in transgenic animals expressing a constitutively active mutant GOA-1^{Q205L} protein that increases $G\alpha_o$ signaling in the HSN neurons, LX2004 *vsIs183 lite-1(ce314) lin-15(n765ts) X* males were crossed with LX849 *vsIs49; lin-15(n765ts) X* hermaphrodites. As above, we noted a repulsion between the *vsIs183* and *vsIs49* transgenes integrated on X. As such, we selected a strain MIA277 with trans-heterozygous *vsIs49* and *vsIs183* transgenes (*lite-1(ce314) vsIs49 X / lite-1(ce314) vsIs183 X*) for Ca^{2+} imaging. The MIA277 strain was maintained by picking phenotypically egg-laying defective adult animals which show GCaMP/mCherry expression.

Vulval Muscle Ca^{2+}: Vulval muscle Ca^{2+} activity was recorded in adult animals using LX1918 *vsIs164* [*unc-103e::GCaMP5::unc-54 3'UTR + unc-103e::mCherry::unc-54 3'UTR + lin-15(+)*] *lite-1(ce314) lin-15(n765ts) X* strain as described (Collins et al., 2016). To visualize vulval muscle activity in $G\alpha_o$ signaling mutants, LX1918 males were crossed with MT2426 *goa-1(n1134)* I, DG1856 *goa-1(sa734) I*, MT8504 *egl-10(md176) V* hermaphrodites, and the fluorescent cross-progeny were allowed to self, generating MIA214 *goa-1(n1134) I; vsIs164 lite-1(ce314) lin-15(n765ts) X*, MIA295 *goa-1(sa734) I*; *vsIs164 lite-1(ce314) lin-15(n765ts) X*, and MIA290 *egl-10(md176)* ; *vsIs164 lite-1(ce314) lin-15(n765ts)* X strains, respectively. To visualize vulval muscle activity in transgenic animals expressing the catalytic subunit of Pertussis Toxin in the HSN neurons (Tanis et al., 2008), MIA218 *vsIs50 lite-1(ce314) lin-15(n765ts) X* males were crossed with LX1919 *vsIs165* [*unc-103e::GCaMP5::unc-54 3'UTR + unc-103e::mCherry::unc-54 3'UTR + lin-15(+)*]*; lite-1(ce314) lin-15(n765ts) X* hermaphrodites, and the cross progeny were allowed to self, generating MIA245 *vsIs50; vsIs165; lite-1(ce314) lin-15(n765ts) X*. To visualize vulval muscle activity in transgenic animals expressing a constitutively active mutant

bioRxiv preprint doi: https://doi.org/10.1101/701664; this version posted July 13, 2019. The copyright holder for this preprint (which was not certified by peer review) is the author/funder, who has granted bioRxiv a license to display the preprint in perpetuity. It is made available under aCC-BY 4.0 International license.

637 GOA-1^{Q205L} protein which increases Gα$_o$ signaling in the HSN neurons (Tanis et al., 2008),
638 LX849 *vsIs49; lin-15(n765ts) X* males were crossed with LX1919 *vsIs165; lite-1(ce314) lin-*
639 *15(n765ts) X* hermaphrodites and the fluorescent cross-progeny were allowed to self, generating
640 MIA291 *vsIs165; vsIs50 lite-1(ce314) lin-15(n765ts) X*.
641
642 Transgenes used to manipulate Gα$_o$ signaling in the HSN neurons, vulval muscles, and uv1
643 neuroendocrine cells
644 ***HSN neurons***: To produce a HSN (and NSM)-specific GPB-1 expressing construct, the *gpb-1*
645 cDNA fragment was amplified from pDEST-*gpb-1* (Yamada et al., 2009) using the following
646 oligonucleotides: 5'- GAGGCTAGCGTAGAAAAAATGAGCGAACTTGACCAACTTCGA-3' and
647 5'-GCGGGTACCTCATTAATTCCAGATCTTGAGGAACGAG-3'. The ~1 kb DNA fragment was
648 digested with NheI/KpnI and ligated into pJT40A (Tanis et al., 2008) to generate pBR30. To
649 produce an HSN (and NSM)-specific GPC-2 expressing construct, the *gpc-2* cDNA fragment
650 was amplified from worm genomic DNA using the following forward and reverse
651 oligonucleotides: 5'-GAGGCTAGCGTAGAAAAAATGGATAAATCTGACATGCAACGA-3' and
652 5'-GCGGGTACCTTAGAGCATGCTGCACTTGCT-3'. The ~250 bp DNA fragment was digested
653 with NheI/KpnI and ligated into pJT40A to generate pBR31. To co-overexpress the βγ G protein
654 subunits in the HSN neurons, we injected pBR30 (50ng/µl), pBR31 (50ng/µl), and pJM60 [*ptph-*
655 *1*::GFP] (80 ng/µl) (Moresco and Koelle, 2004) into the LX1832 *lite-1(ce314) lin-15(n765ts)*
656 animals along with pLI5EK (50 ng/µl), generating five independent extrachromosomal transgenic
657 lines which were used for behavioral assays. One representative transgenic strain, MIA278
658 [*keyEx52*; *lite-1(ce314) lin-15(n765ts)*], was kept. To generate a control strain for comparison in
659 the egg-laying assays, we injected pJM66 [*ptph-1*::empty] (100 ng/µl) (Tanis et al., 2008) and
660 pJM60 (80 ng/µl) into the LX1832 *lite-1(ce314) lin-15(n765ts)* animals along with pLI5EK (50
661 ng/µl) generating five independent extrachromosomal control transgenes which were used for

bioRxiv preprint doi: https://doi.org/10.1101/701664; this version posted July 13, 2019. The copyright holder for this preprint (which was not certified by peer review) is the author/funder, who has granted bioRxiv a license to display the preprint in perpetuity. It is made available under aCC-BY 4.0 International license.

behavioral assays. One representative transgenic strain, MIA279 [*keyEx53*; *lite-1(ce314) lin-15(n765ts)*], was kept.

Vulval muscles: pJT40A (*ptph-1*::Pertussis Toxin (Tanis et al., 2008) was digested with NheI/KpnI and ligated into pBR3 (*pceh-24*::mCherry) to generate pBR20. pBR20 [*pceh-24*::Pertussis Toxin] (10 ng/µl) and pBR3 [*pceh-24*::mCherry] (10 ng/µl) were injected into the LX1832 *lite-1(ce314) lin-15(n765ts)* animals along with pLI5EK (50 ng/µl) to generate five independent extrachromosomal transgenes which were used for behavioral assays. One representative transgenic strain, MIA257 [*keyEx46*; *lite-1(ce314) lin-15(n765ts)*], was kept. To produce vulval muscle-specific GOA-1(Q205L), the coding sequence of GOA-1(Q205L) was recovered from pJM70C (Tanis et al., 2008) after digestion with NheI/SacI and ligated into pKMC188 (*punc-103e*::GFP; (Collins and Koelle, 2013)) generating pKMC268 (*punc-103e::goa-1(Q205L)*). However, because the *unc-103e* promoter also directs expression in neurons that might indirectly regulate egg laying, GOA-1(Q205L) coding sequences were removed from pKMC268 by digesting with NheI/NcoI and ligated into pBR3 to generate pBR21. pBR21 [*pceh-24*::GOA-1^{Q205L}] (10 ng/µl) and pBR3 [*pceh-24*::mCherry] (10 ng/µl) were injected into the LX1832 *lite-1(ce314) lin-15(n765ts)* animals along with pLI5EK (50 ng/µl) to generate five independent extrachromosomal transgenes which were used for behavior assays. One representative transgenic strain, MIA258 [*keyEx47*; *lite-1(ce314) lin-15(n765ts)*], was kept. To generate control strains for comparison in egg-laying assays, pBR3 [*pceh-24*::mCherry] (20 ng/µl) was injected into the LX1832 *lite-1(ce314) lin-15(n765ts)* animals along with pLI5EK (50 ng/µl) to generate five independent extrachromosomal transgenes which were used for behavioral assays. One representative control transgenic strain, MIA256 [*keyEx45*; *lite-1(ce314) lin-15(n765ts)*], was kept. To produce a vulval muscle-specific Tetanus Toxin transgene, Tetanus Toxin coding sequences were amplified from pAJ49 (*pocr-2*::Tetanus toxin) (Jose et al., 2007) using the following oligonucleotides: 5'-

bioRxiv preprint doi: https://doi.org/10.1101/701664; this version posted July 13, 2019. The copyright holder for this preprint (which was not certified by peer review) is the author/funder, who has granted bioRxiv a license to display the preprint in perpetuity. It is made available under aCC-BY 4.0 International license.

GAGGCTAGCGTAGAAAAAATGCCGATCACCATCAACAACTTC-3' and 5'-GCGCAGGCGGCCGCTCAAGCGGTACGGTTGTACAGGTT-3'. The DNA fragment was digested with NheI/NotI and ligated into pBR6 to generate pBR27. To block any possible neurotransmitter release from the vulval muscles, pBR27 (10 ng/µl) and pBR3 (10 ng/µl) was injected into the LX1832 *lite-1(ce314) lin-15(n765ts)* animals along with pLI5EK (50 ng/µl) to generate five independent extrachromosomal transgenes which were used for behavior assays. One representative transgenic strain, MIA262 [*keyEx51*; *lite-1(ce314) lin-15(n765ts)*], was kept.

uv1 neuroendocrine cells*:* To generate a uv1 cell-specific Pertussis toxin transgene, pBR20 (*pceh-24*::Pertussis toxin) was digested with NheI/NcoI and the coding sequences of Pertussis Toxin were then ligated into pAB5 (*ptdc-1*::mCherry::*ocr-2* 3'UTR) to generate pBR25. pBR25 [*ptdc-1*::Pertussis Toxin] (10 ng/µl) and pAB5 [*ptdc-1*::mCherry] (5 ng/µl) were injected into LX1832 *lite-1(ce314) lin-15(n765ts)* animals along with pLI5EK (50 ng/µl) to generate five independent extrachromosomal transgenes which were used for behavioral assays. One representative transgenic strain, MIA260 [*keyEx49*; *lite-1(ce314) lin-15(n765ts)*], was kept. To generate a uv1 cell-specific GOA-1(Q205L) transgene, pKMC268 (*punc-103e*::GOA-1(Q205L)) was digested with NheI/NcoI and the coding sequences of GOA-1(Q205L) were then ligated into pBR25 to generate pBR26. To increase $G\alpha_o$ signaling in uv1 cells, we injected pBR26 [*ptdc-1*::GOA-1^{Q205L}] (10 ng/µl) and pAB5 [*ptdc-1*::mCherry] (5 ng/µl) into the LX1832 *lite-1(ce314) lin-15(n765ts)* animals along with pLI5EK (50 ng/µl) to generate five independent extrachromosomal transgenes which were used for behavioral assays. One transgenic strain MIA261 [*keyEx50*; *lite-1(ce314) lin-15(n765ts)*] was kept. To generate a control strain for comparison in our egg-laying assays, pAB5 [*ptdc-1*::mCherry] (15 ng/µl) was injected into the LX1832 *lite-1(ce314) lin-15(n765ts)* animals along with pLI5EK (50 ng/µl) to generate five independent extrachromosomal transgenes which were used for behavioral assays. One representative transgenic strain, MIA259 [*keyEx48*; *lite-1(ce314) lin-15(n765ts)*], was kept.

bioRxiv preprint doi: https://doi.org/10.1101/701664; this version posted July 13, 2019. The copyright holder for this preprint (which was not certified by peer review) is the author/funder, who has granted bioRxiv a license to display the preprint in perpetuity. It is made available under aCC-BY 4.0 International license.

Fluorescence Imaging

Ratiometric Ca^{2+} Imaging: Ratiometric Ca^{2+} recordings were performed on freely behaving animals mounted between a glass coverslip and chunk of NGM agar, as previously described (Collins and Koelle, 2013; Li et al., 2013; Collins et al., 2016; Ravi et al., 2018b). Briefly, recordings were collected on an inverted Leica TCS SP5 confocal microscope using the 8 kHz resonant scanner at ~20 fps at 256x256 pixel resolution, 12-bit depth and ≥2X digital zoom using a 20x Apochromat objective (0.7 NA) with the pinhole opened to ~20 µm. GCaMP5G and mCherry fluorescence was excited using a 488 nm and 561 nm laser lines, respectively. Adult recordings were performed 24 hours after the late L4 stage. After staging, animals were allowed to adapt for ~30 min before imaging. During imaging, the stage and focus were adjusted manually to keep the relevant cell/pre-synapse in view and in focus.

Ratiometric analysis (GCaMP5:mCherry) for all Ca^{2+} recordings was performed after background subtraction using Volocity 6.3.1 as described (Collins et al., 2016; Ravi et al., 2018a). The egg-laying active state was operationally defined as the period one minute prior to the first egg-laying event and ending one minute after the last (in the case of a typical active phase where 3-4 eggs are laid in quick succession). However, in cases where two egg-laying events were apart by >60 s, peaks were considered to be in separate active phases and any transients observed between were considered to be from an inactive state. In animals where we observed no Ca^{2+} peaks during the entire recording, the total duration of the recording was considered an inter-transient interval. In animals where we observed a single Ca^{2+} transient, the duration from the start of the recording to the time of the Ca^{2+} transient and the time from the Ca^{2+} transient to the end of the recording were counted as inter-transient intervals.

bioRxiv preprint doi: https://doi.org/10.1101/701664; this version posted July 13, 2019. The copyright holder for this preprint (which was not certified by peer review) is the author/funder, who has granted bioRxiv a license to display the preprint in perpetuity. It is made available under aCC-BY 4.0 International license.

Behavior Assays and Microscopy

Animal sterilization: Animals were sterilized using Floxuridine (FUDR). Briefly, 100 µl of 10 mg/ml FUDR was applied to OP50 seeded NGM plates. Late L4 animals were then staged onto the FUDR plates and the treated adults were imaged 24 hours later.

Egg laying assays: Unlaid eggs were quantitated as described (Chase et al., 2004). Staged adults were obtained by picking late L4 animals and culturing them for 30-40 hr at 20°C. The percentage of early-stage eggs laid were quantified as described (Koelle and Horvitz, 1996). 30 staged adults were placed on a thin lawn of OP50 bacteria on a nematode growth medium (NGM) agar plate (Brenner, 1974) and allowed to lay eggs for 30 min. This was repeated with new sets of staged animals until a total of at least 100 laid eggs were analyzed. Each egg was examined under a Leica M165FC stereomicroscope and categorized into the following categories: eggs which have 1 cell, 2 cell, 3-4 cell, 5-8 cell, and embryos with >8 cells. Eggs with eight cells or fewer were classified as “early stage.”

Long-term recording of egg-laying behavior: Egg-laying behavior was recorded at 4-5 frames per second from 24-hour adults after transfer to NGM plates seeded with a thin lawn of OP50 bacterial food using a Leica M165FC stereomicroscope and camera (Grasshopper 3, 4.1 Megapixel, USB3 CMOS camera, Point Grey Research). N2 wild-type and hyperactive egg-laying mutant strains (MT2426 and LX850) were recorded for 3 hours, and the egg-laying defective strains MT8504 and LX849 were recorded for 8-10 hours.

Electrophysiology

Electrophysiological recordings were carried out on an upright microscope (Olympus BX51WI) coupled with an EPC-10 amplifier and Patchmaster software (HEKA), as previously described

bioRxiv preprint doi: https://doi.org/10.1101/701664; this version posted July 13, 2019. The copyright holder for this preprint (which was not certified by peer review) is the author/funder, who has granted bioRxiv a license to display the preprint in perpetuity. It is made available under aCC-BY 4.0 International license.

(Yue et al., 2018; Zou et al., 2018). Briefly, day 2 adult worms were glued on the surface of Sylgard-coated coverslips using the cyanoacrylate-based glue (Gluture Topical Tissue Adhesive, Abbott Laboratories). A dorsolateral incision was made using a sharp glass pipette to expose the cell bodies of HSN neurons for recording. The bath solution contained (in mM) 145 NaCl, 2.5 KCl, 5 $CaCl_2$, 1 $MgCl_2$, and 20 glucose (325–335 mOsm, pH adjusted to 7.3). The pipette solution contained (in mM) 145 KCl, 5 $MgCl_2$, 5 EGTA, 0.25 $CaCl_2$, 10 HEPES, 10 glucose, 5 Na_2ATP and 0.5 NaGTP (315–325 mOsm, pH adjusted to 7.2) The resting membrane potentials were tested with 0 pA holding under the Current Clamp model of whole-cell patch.

Experimental Design and Statistical Analysis

Sample sizes for behavioral assays followed previous studies (Chase et al., 2004; Collins and Koelle, 2013; Collins et al., 2016). No explicit power analysis was performed before the study. Statistical analysis was performed using Prism 6 (GraphPad). Ca^{2+} transient peak amplitudes and inter-transient intervals were pooled from multiple animals (typically ~10 animals per genotype/condition per experiment). No animals or data were excluded. Individual *p* values are indicated in each Figure legend, and all tests were corrected for multiple comparisons (Bonferroni for ANOVA and Fisher exact test; Dunn for Kruskal-Wallis).

Disclosures / Conflict of Interests

The authors declare no conflicts of interest.

bioRxiv preprint doi: https://doi.org/10.1101/701664; this version posted July 13, 2019. The copyright holder for this preprint (which was not certified by peer review) is the author/funder, who has granted bioRxiv a license to display the preprint in perpetuity. It is made available under aCC-BY 4.0 International license.

Acknowledgements

This work was funded by grants from the NIH (R01-NS086932) and NSF (IOS-1844657) to KMC. Strains used in this study have been provided to the *C. elegans* Genetics Center, which is funded by NIH Office of Research Infrastructure Programs (P40 OD010440). We thank Addys Bode Hernandez for expert technical assistance. We thank James Baker, Julia Dallman, Laura Bianchi, Brock Grill, Peter Larsson, Mason Klein, Stephen Roper, and members of the Collins lab for helpful discussions and feedback on the manuscript.

bioRxiv preprint doi: https://doi.org/10.1101/701664; this version posted July 13, 2019. The copyright holder for this preprint (which was not certified by peer review) is the author/funder, who has granted bioRxiv a license to display the preprint in perpetuity. It is made available under aCC-BY 4.0 International license.

Figures

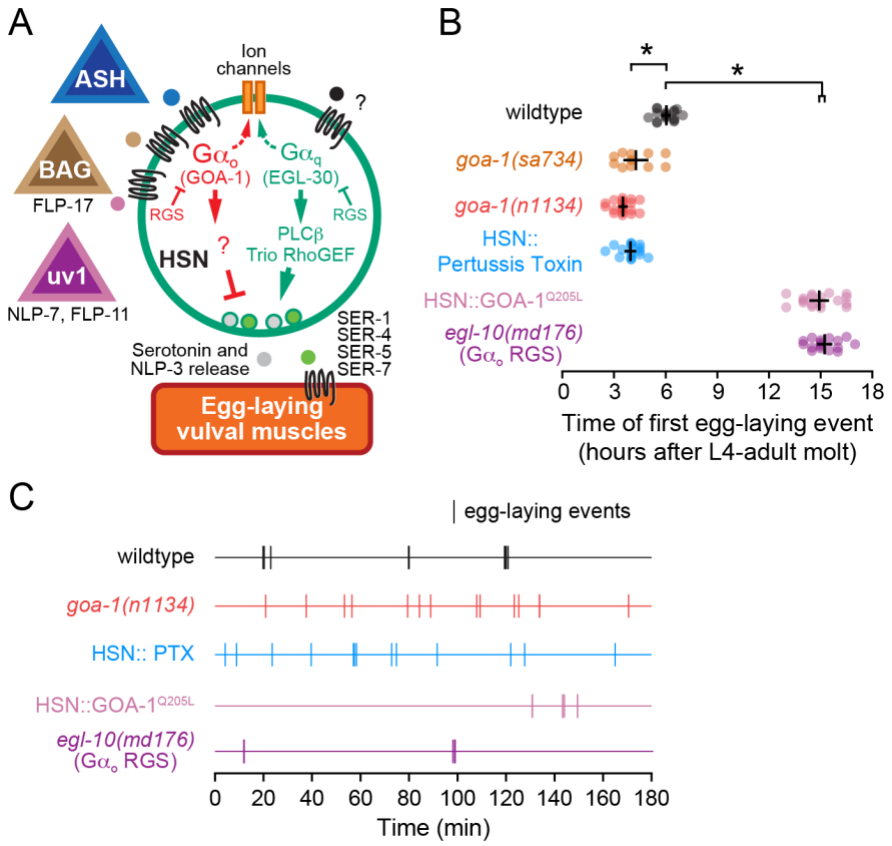

Figure 1. Gα$_o$ signaling maintains the inactive egg-laying behavior state.

(**A**) Cartoon of how neuropeptides released from ASH, BAG, and uv1 sensory cells bind to G-protein coupled receptors expressed on HSN command neurons (green) which signal via Gα$_o$ or Gα$_q$ effector pathways to modulate HSN excitability and neurotransmitter release. The egg-laying vulval muscles (orange) express receptors for serotonin and possibly NLP-3 which signal to promote vulval muscle excitability and egg laying (**B**) Scatter plots of the first egg-laying event in wildtype (grey), null *goa-1(sa734)* mutants (orange), hypomorphic loss-of-function *goa-1(n1134)* mutants (red), *egl-10(md176)* null mutants (purple), and transgenic animals expressing Pertussis Toxin (blue) and GOA-1^{Q205L} in the HSNs (pink). Error bars show 95% confidence intervals for the mean from ≥10 animals. Asterisks indicate p≤0.0001 (One-way ANOVA with Bonferroni correction for multiple comparisons). (**C**) Representative raster plots showing

bioRxiv preprint doi: https://doi.org/10.1101/701664; this version posted July 13, 2019. The copyright holder for this preprint (which was not certified by peer review) is the author/funder, who has granted bioRxiv a license to display the preprint in perpetuity. It is made available under aCC-BY 4.0 International license.

temporal pattern of egg laying during three hours in wild-type (black), hypomorphic loss-of-function *goa-1(n1134)* mutant (red), and *egl-10(md176)* null mutant animals (purple), along with transgenic animals expressing Pertussis Toxin (blue) and GOA-1^{Q205L} in the HSNs (pink). Vertical lines indicate single egg-laying events.

bioRxiv preprint doi: https://doi.org/10.1101/701664; this version posted July 13, 2019. The copyright holder for this preprint (which was not certified by peer review) is the author/funder, who has granted bioRxiv a license to display the preprint in perpetuity. It is made available under aCC-BY 4.0 International license.

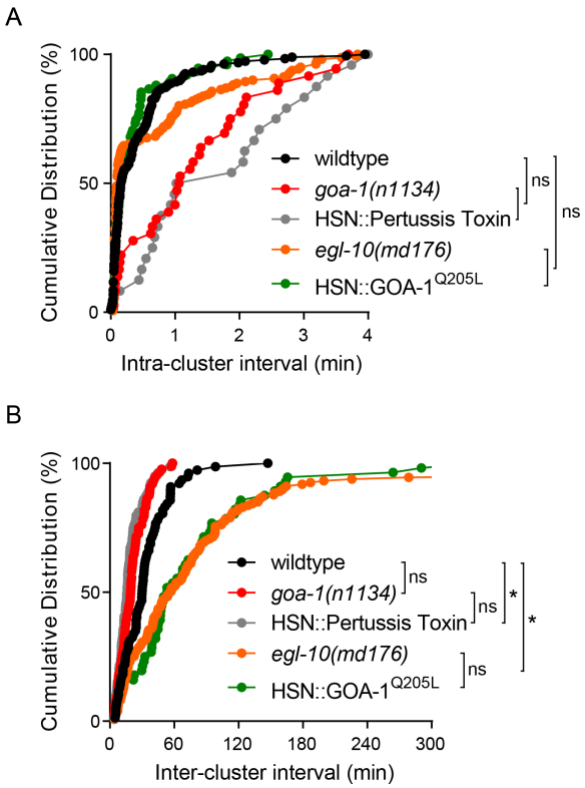

Figure 1–figure supplement 1. Gα$_o$ signaling prolongs the interval between egg-laying active states.

(**A**) and (**B**) Cumulative distributions of intra-cluster and inter-cluster intervals in wild-type (black), *goa-1(n1134)* mutant (red), and *egl-10(md176)* (orange) mutant animals, along with transgenic animals expressing Pertussis Toxin (grey) or activated GOA-1^{Q205L} (green) in HSN from the *tph-1* gene promoter. Intra-cluster intervals are operationally defined as those intervals between egg-laying events being <4 minutes while inter-cluster intervals are defined as those intervals between egg-laying events being >4 minutes duration. Asterisks indicate p<0.0001 (Kruskal-Wallis test with Dunn's correction for multiple comparisons). N≥10 animals were analyzed per genotype. Total intra-cluster intervals (intervals <4 minutes) used for analysis in (A) for each strain were as follows: wildtype (n=188), *goa-1(n1134)* mutants (n=36), HSN::Pertussis toxin transgenic animals (n=24), *egl-10(md176)* null mutants (n=161), and HSN::GOA-1^{Q205L} transgenic animals (n=75). Total inter-cluster intervals (intervals >4 minutes) used for analysis

bioRxiv preprint doi: https://doi.org/10.1101/701664; this version posted July 13, 2019. The copyright holder for this preprint (which was not certified by peer review) is the author/funder, who has granted bioRxiv a license to display the preprint in perpetuity. It is made available under aCC-BY 4.0 International license.

in (B) for each strain were as follows: wildtype (n=77), hypomorphic *goa-1(n1134)* mutants (n=88), HSN::Pertussis toxin transgenic animals (n=79), *egl-10(md176)* null mutants (n=147), and HSN::GOA-1^{Q205L} transgenic animals (n=56).

bioRxiv preprint doi: https://doi.org/10.1101/701664; this version posted July 13, 2019. The copyright holder for this preprint (which was not certified by peer review) is the author/funder, who has granted bioRxiv a license to display the preprint in perpetuity. It is made available under aCC-BY 4.0 International license.

Genotype Genotype	***Intra*-cluster interval ($1/\lambda_1$)** Average (min) (95%CI range)	***Inter*-cluster interval ($1/\lambda_2$)** Average (min) (95%CI range)	**Eggs laid per per active state** Average ± 95%CI	**Unlaid eggs per animal** Average ± 95%CI
Wildtype	0.42 (0.33-0.51)	22.11 (21.19-23.09)	2.5 ± 0.5	15.9 ± 1.5
goa-1(n1134)	1.31 (0.94-1.67)	12.88* (12.31-12.75)	1.2 ± 0.1‡	2.2 ± 0.3
HSN::Pertussis Toxin	1.69 (1.17-2.20)	12.42* (12.09-12.75)	1.1 ± 0.07‡	4.1 ± 0.3 ##
egl-10(md176)	0.64 (0.49-0.79)	258.6* (231.26-293.42)	2.5 ± 0.2	45.9 ± 3.3
HSN::GOA-1^{Q205L}	0.35 (0.24-0.47)	66.97* (64.14-70.02)	2.2 ± 0.2	36.8 ± 3.8

Table 1. Egg-laying behavior measurements in animals with altered $G\alpha_o$ signaling.

Long-term behavior recordings were used to extract features of egg-laying active and inactive behavior states for the indicated genotypes, as described (Figure 1-figure supplement 1) (Waggoner et al., 1998). Asterisks indicate significant differences compared to wildtype ($p<0.0001$, Kruskal-Wallis test with Dunn's correction for multiple comparisons). '‡' indicates significant differences compared to wildtype ($p<0.0001$, One-way ANOVA with Bonferroni correction). ## indicates that this result was previously reported (Tanis et al., 2008).

bioRxiv preprint doi: https://doi.org/10.1101/701664; this version posted July 13, 2019. The copyright holder for this preprint (which was not certified by peer review) is the author/funder, who has granted bioRxiv a license to display the preprint in perpetuity. It is made available under aCC-BY 4.0 International license.

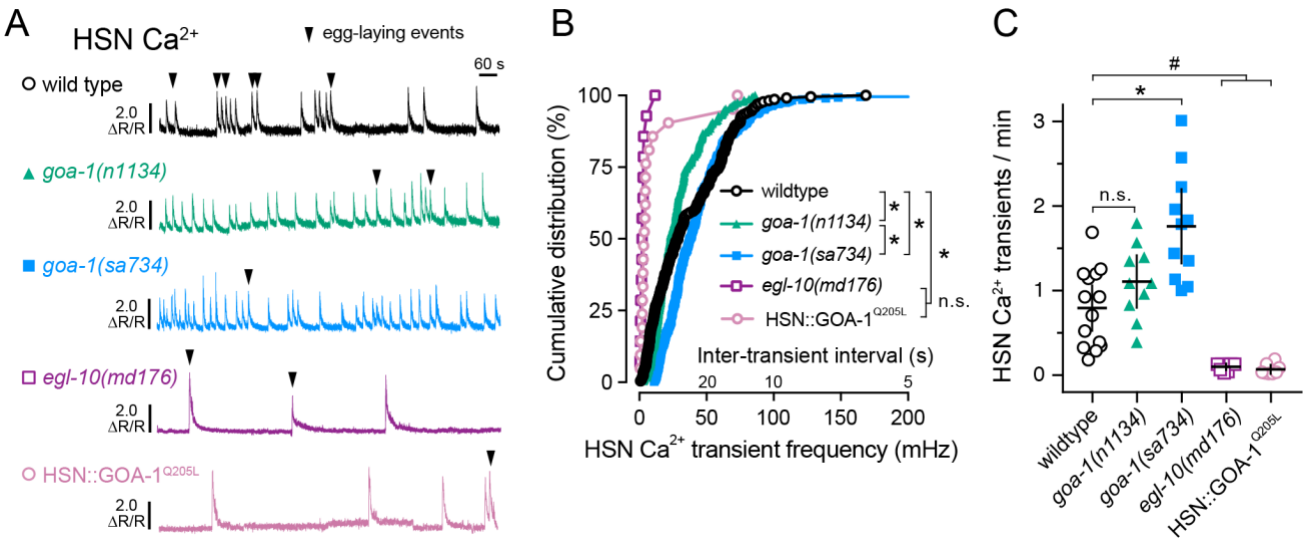

Figure 2. Gα$_o$ signaling inhibits HSN neuron Ca^{2+} activity and burst firing.

(**A**) Representative GCaMP5:mCherry (ΔR/R) ratio traces showing HSN Ca^{2+} activity in freely behaving wild-type (black), *goa-1(n1134)* loss-of-function mutant (green), *goa-1(sa734)* null mutant (blue), and *egl-10(md176)* null (purple) mutant animals, along with transgenic animals expressing the activated GOA-1(Q205L) in the HSN neurons (pink) during an egg-laying active state. Arrowheads indicate egg-laying events. (**B**) Cumulative distribution plots of instantaneous Ca^{2+} transient peak frequencies (and inter-transient intervals) in wild-type (black open circles), *goa-1(n1134)* (green filled triangles), *goa-1(sa734)* (blue squares), *egl-10(md176)* mutants (purple open squares) along with transgenic animals expressing the activated GOA-1(Q205L) in the HSN neurons (pink open circles). Asterisks indicate $p<0.0001$ (Kruskal-Wallis test with Dunn's correction for multiple comparisons). (**C**) Scatter plots show average Ca^{2+} transient frequency (per min) in wild-type (black open circles), *goa-1(n1134)* (green filled triangles), *goa-1(sa734)* (blue filled squares), *egl-10(md176)* mutants (purple open circles), and transgenic animals expressing GOA-1(Q205L) in the HSN neurons (pink open circles). Error bars indicate 95% confidence intervals for the mean. Asterisk indicates $p<0.0001$; pound (#) indicates $p\leq0.0079$; n.s. indicates $p>0.05$ (One-way ANOVA with Bonferroni correction for multiple comparisons).

bioRxiv preprint doi: https://doi.org/10.1101/701664; this version posted July 13, 2019. The copyright holder for this preprint (which was not certified by peer review) is the author/funder, who has granted bioRxiv a license to display the preprint in perpetuity. It is made available under aCC-BY 4.0 International license.

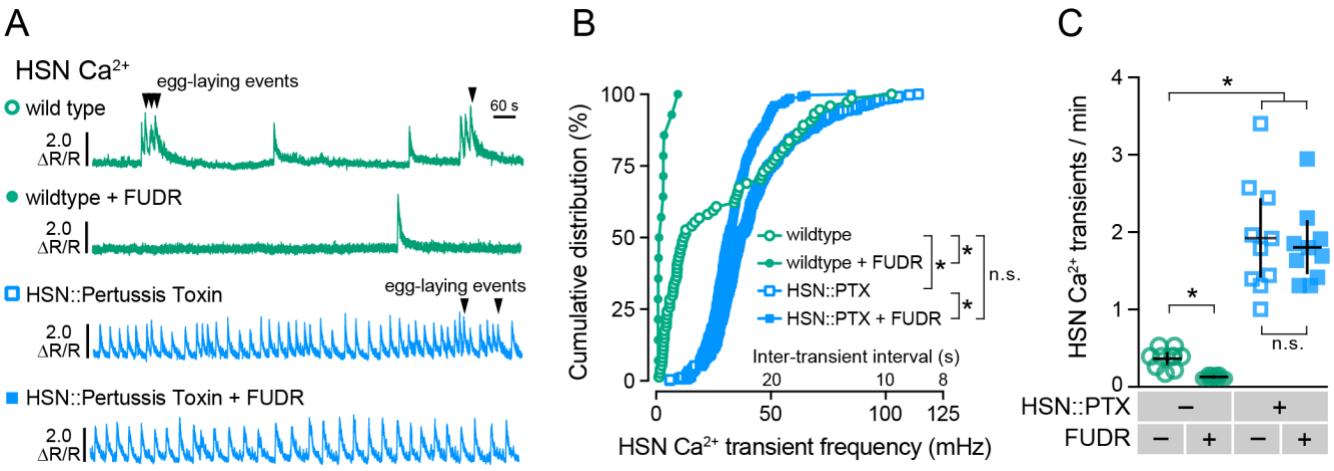

Figure 3. Inhibitory Gα$_o$ signaling in HSN is required for two-state Ca^{2+} activity and facilitates modulation by the homeostat.

(A) Representative GCaMP5:mCherry (ΔR/R) ratio traces showing HSN Ca^{2+} activity in untreated fertile wild-type animals (green, top), FUDR-sterilized wild-type animals (green, bottom), untreated fertile animals expressing Pertussis Toxin (PTX) in the HSN neurons (blue, top), and in FUDR-sterilized transgenic animals expressing PTX in the HSNs (blue, bottom). Arrowheads indicate egg-laying events. (**B**) Cumulative distribution plots of instantaneous Ca^{2+} transient peak frequencies (and inter-transient intervals) in untreated (open circles) and FUDR-treated (filled circles) wild-type control (blue) and Pertussis Toxin expressing transgenic animals (green). Asterisks indicate $p<0.0001$ (Kruskal-Wallis test with Dunn's test for multiple comparisons). (**C**) Scatter plots show average Ca^{2+} transient frequency (per min) in untreated (open circles) and FUDR-treated (filled circles) wild-type control (blue) and Pertussis Toxin expressing transgenic animals (green). Error bars indicate 95% confidence intervals for the mean. Asterisks indicate $p<0.0001$ (One-way ANOVA with Bonferroni's test for multiple comparisons). Data from 10 animals were used for each strain for analysis.

bioRxiv preprint doi: https://doi.org/10.1101/701664; this version posted July 13, 2019. The copyright holder for this preprint (which was not certified by peer review) is the author/funder, who has granted bioRxiv a license to display the preprint in perpetuity. It is made available under aCC-BY 4.0 International license.

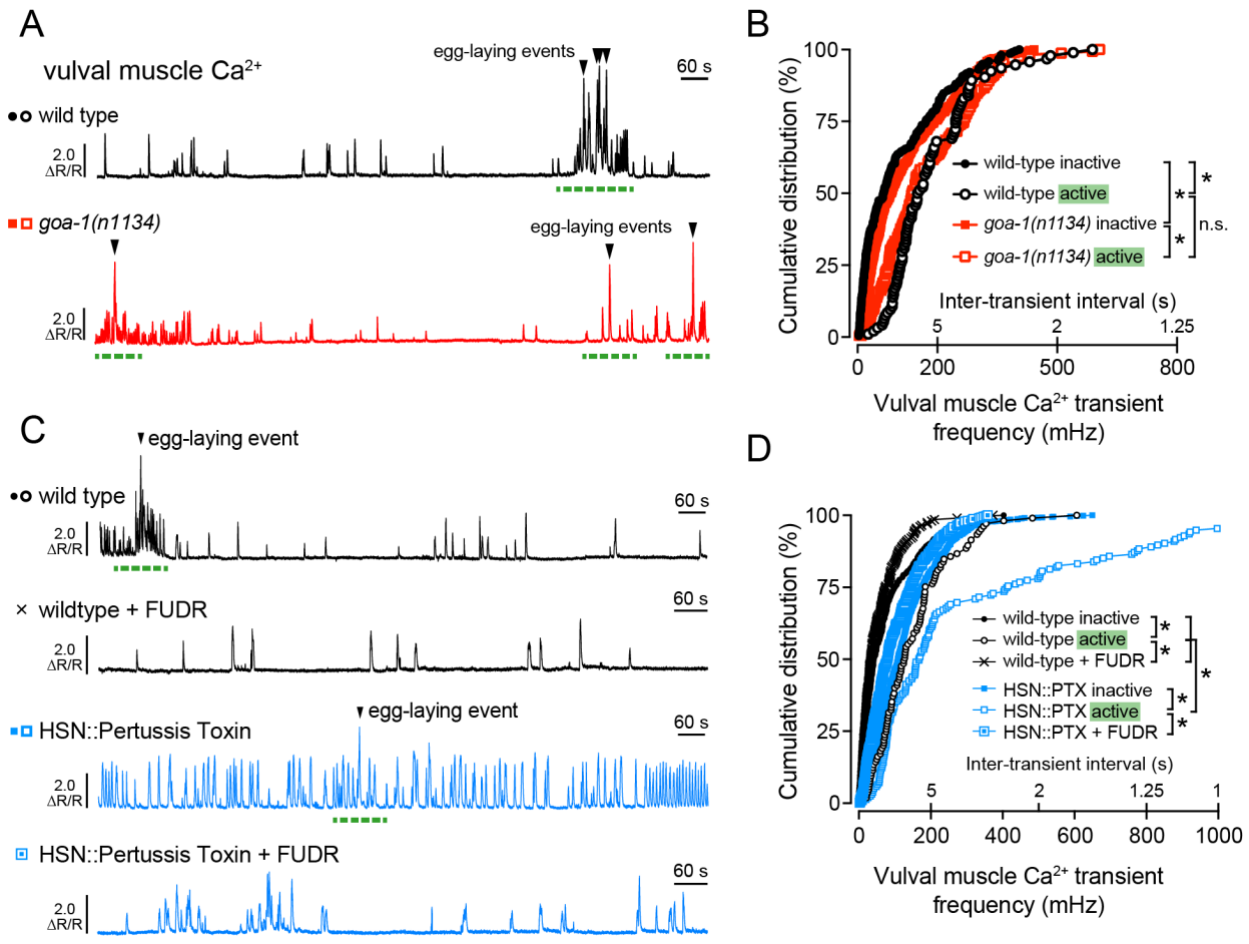

Figure 4. Gα$_o$ signals in HSN to reduce excitatory modulation of the vulval muscles.

(A) Representative GCaMP5:mCherry (ΔR/R) ratio traces showing vulval muscle Ca^{2+} activity in wild-type (black) and *goa-1(n1134)* loss-of-function mutant animals (red). Egg-laying events are indicated by arrowheads, and egg-laying active states are indicated by dashed green lines. **(B)** Cumulative distribution plots of instantaneous vulval muscle Ca^{2+} transient peak frequencies (and inter-transient intervals) in wild-type (black circles) and *goa-1(n1134)* mutant animals (red squares) in the egg-laying inactive and active states (filled and open, respectively). **(C)** Representative GCaMP5:mCherry (ΔR/R) ratio traces showing vulval muscle Ca^{2+} activity in untreated (circles) and FUDR-treated (cross) wild-type animals (black) along with untreated (filled) or FUDR-treated (open) transgenic animals expressing Pertussis Toxin in the HSNs (blue

bioRxiv preprint doi: https://doi.org/10.1101/701664; this version posted July 13, 2019. The copyright holder for this preprint (which was not certified by peer review) is the author/funder, who has granted bioRxiv a license to display the preprint in perpetuity. It is made available under aCC-BY 4.0 International license.

881 squares). Egg-laying events are indicated by arrowheads, and egg-laying active states are
882 indicated by green dashed lines. **(D)** Cumulative distribution plots of instantaneous vulval muscle
883 Ca^{2+} transient peak frequencies (and inter-transient intervals) in wildtype and in transgenic
884 animals expressing Pertussis Toxin in the HSN neurons. Asterisks indicate $p<0.0001$ (Kruskal-
885 Wallis test with Dunn's test for multiple comparisons).

886

bioRxiv preprint doi: https://doi.org/10.1101/701664; this version posted July 13, 2019. The copyright holder for this preprint (which was not certified by peer review) is the author/funder, who has granted bioRxiv a license to display the preprint in perpetuity. It is made available under aCC-BY 4.0 International license.

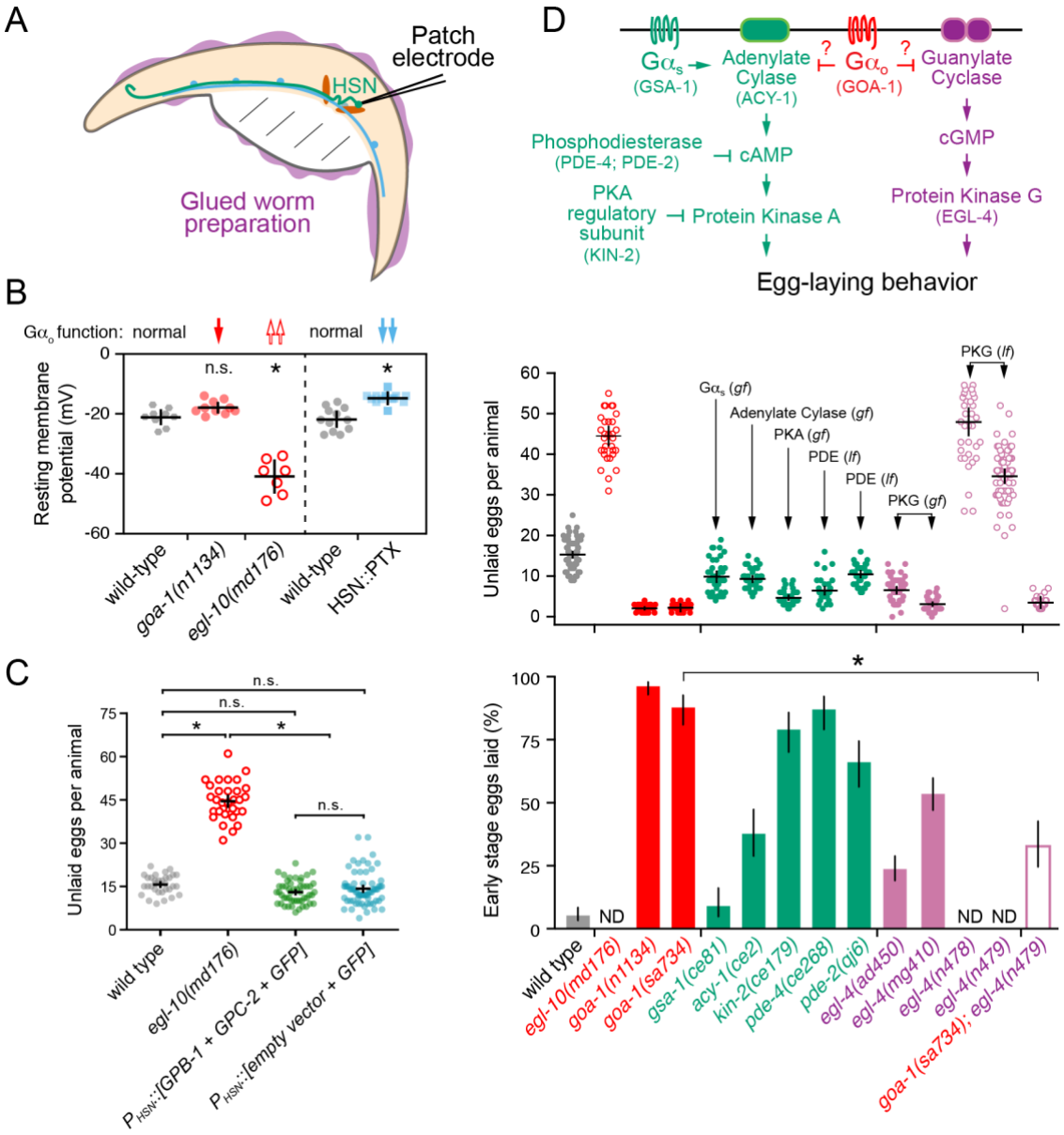

Figure 5. Gα$_o$ depresses HSN resting membrane potential and may regulate egg-laying behavior via modulation of cGMP and cAMP signaling pathways.

(**A**) Cartoon of the 'fileted' worm preparation used for patch clamp electrophysiology of HSN. (**B**) Scatter plots show resting membrane potential of wild-type control animals (grey circles), *goa-1(n1134)* loss-of-function mutants (red filled circles), *egl-10(md176)* null mutants (red open circles), and in transgenic animals expressing Pertussis Toxin in HSN (blue filled squares). Error bars indicate 95% confidence intervals for the mean. Asterisks indicate p<0.0001 (One-Way

bioRxiv preprint doi: https://doi.org/10.1101/701664; this version posted July 13, 2019. The copyright holder for this preprint (which was not certified by peer review) is the author/funder, who has granted bioRxiv a license to display the preprint in perpetuity. It is made available under aCC-BY 4.0 International license.

ANOVA with Bonferroni correction for multiple comparisons). N≥7 animals recorded per genotype. (**C**) Scatter plots show average number of eggs retained by wild-type animals (gray filled circles), *egl-10(md176)* null mutants (orange open circles), and in transgenic animals expressing either Gβ (GPB-2) and Gγ (GPC-1) subunits (green filled circles) or nothing (blue filled circles) from the *tph-1* gene promoter along with GFP. Error bars indicate means with 95% confidence intervals. Asterisk indicates $p<0.0001$; n.s. indicates $p>0.05$ (One-Way ANOVA with Bonferroni correction for multiple corrections). (**D**) Top, cartoon of cAMP and cGMP signaling pathways and how they might be inhibited by $G\alpha_o$ signaling. Gene names for *C. elegans* orthologs tested here are indicated in parentheses. Middle, scatterplots show average number of eggs retained by wildtype (grey), *egl-10(md176)* (red open circles), *goa-1(n1134)* and *goa-1(sa734)* $G\alpha_o$ loss of function (red filled circles) mutants, and in animals with altered cAMP effector signaling (green): *gsa-1(ce81)* $G\alpha_s$ gain-of-function, *acy-1(ce2)* Adenylate Cyclase gain-of-function, *kin-2(ce179)* Protein Kinase A (PKA) inhibitory regulatory subunit loss-of-function, *pde-4(ce268)* Phosphodiesterase (PDE) loss-of-function, *pde-2(qj6)* Phosphodiesterase (PDE) null; altered cGMP effector signaling (pink): *egl-4(ad805)* and *egl-4(mg410)* Protein Kinase G (PKG) gain-of-function (pink filled circles), *egl-4(n478)* and *egl-4(n479)* loss-of-function mutants (pink open circles). Bottom, bar graphs indicate percent of embryos laid at early stages of development. N.D. indicates the stages of eggs laid was not determined because those mutants are egg-laying defective (Egl). Error bars indicate 95% confidence intervals for the mean. Asterisk indicates highlighted significant differences ($p\leq0.0001$; Fisher Exact Test).

bioRxiv preprint doi: https://doi.org/10.1101/701664; this version posted July 13, 2019. The copyright holder for this preprint (which was not certified by peer review) is the author/funder, who has granted bioRxiv a license to display the preprint in perpetuity. It is made available under aCC-BY 4.0 International license.

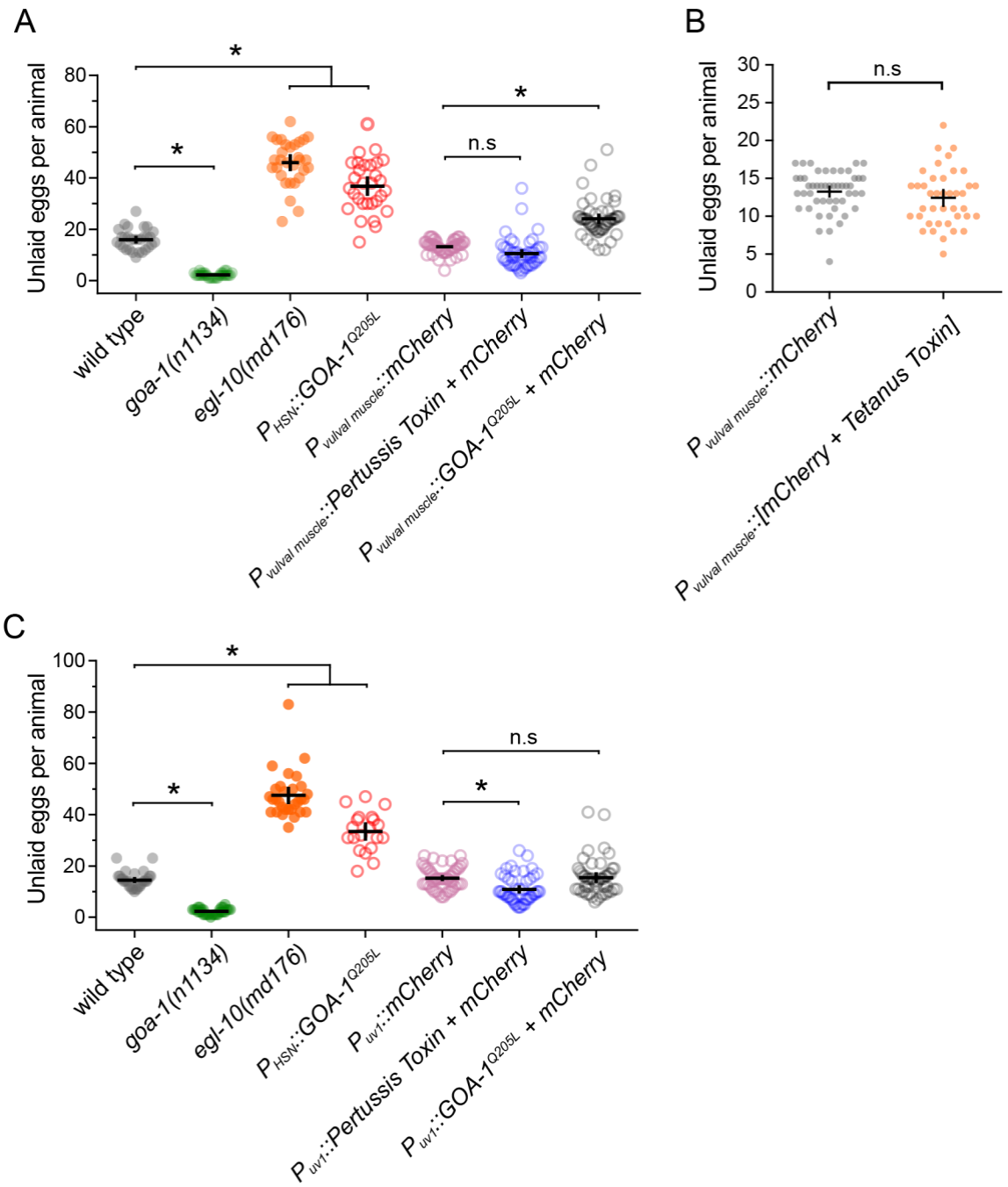

Figure 5–supplemental figure 1. Gα$_o$ signaling in the vulval muscles and uv1 neuroendocrine cells also regulates egg laying.

(A) Scatter plots show average number of eggs retained by wild-type (grey), *goa-1(n1134)* mutants (green), *egl-10(md176)* null mutant animals (orange) along with transgenic animals expressing GOA-1^{Q205L} in the HSNs (red open circles), transgenic animals expressing mCherry

bioRxiv preprint doi: https://doi.org/10.1101/701664; this version posted July 13, 2019. The copyright holder for this preprint (which was not certified by peer review) is the author/funder, who has granted bioRxiv a license to display the preprint in perpetuity. It is made available under aCC-BY 4.0 International license.

(pink open circles), Pertussis Toxin (blue open circles), or GOA-1^{Q205L} (black open circles) in the vulval muscles from the *ceh-24* gene promoter. (**B**) Scatter plots show average number of eggs retrained in transgenic animals expressing only mCherry (gray) or Tetanus Toxin along with mCherry (orange) in the vulval muscles using the *ceh-24* gene promoter. Error bars indicate means with 95% confidence intervals. P=0.2197 (Student's t test). (**C**) Scatter plots show average number of eggs retained by wild-type (grey), *goa-1(n1134)* mutant (green), *egl-10(md176)* null mutant (orange) animals along with transgenic animals expressing GOA-1^{Q205L} in the HSNs (red), transgenic animals expressing mCherry (pink), Pertussis Toxin (blue), or GOA-1^{Q205L} (black open circles) in the uv1 neuroendocrine cells from the *tdc-1* gene promoter. Four or five independent extrachromosomal arrays were generated for each transgene in **(A-C)** and ~10 animals from each extrachromosomal array were used. Error bars indicate 95% confidence intervals for the mean. Asterisks indicate p<0.0001 (One-Way ANOVA with Bonferroni's correction for multiple comparisons).

bioRxiv preprint doi: https://doi.org/10.1101/701664; this version posted July 13, 2019. The copyright holder for this preprint (which was not certified by peer review) is the author/funder, who has granted bioRxiv a license to display the preprint in perpetuity. It is made available under aCC-BY 4.0 International license.

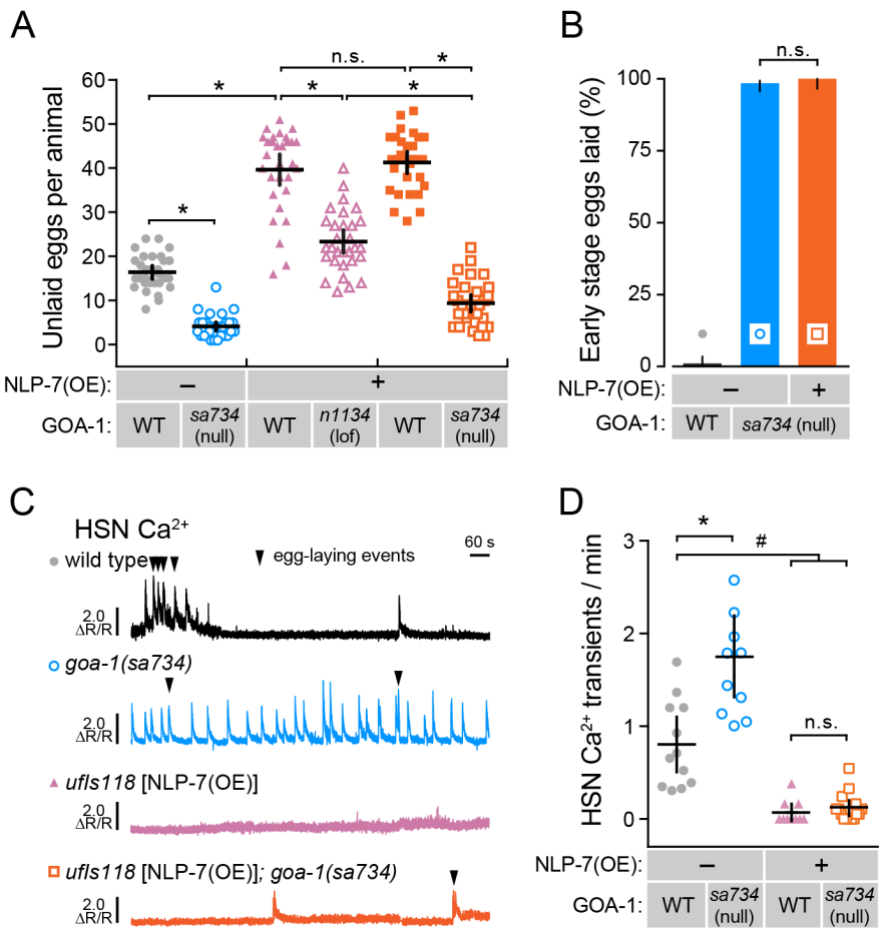

938

939 **Figure 6. NLP-7 neuropeptides signal through Gα$_o$ to inhibit egg-laying independent of**

940 **the HSN neurons**

941 **(A)** NLP-7 signals through Gα$_o$ to suppress egg laying. Scatter plots show average number of

942 eggs retained by wild-type (gray circles), *goa-1(sa734)* mutants (blue open circles), NLP-7 over-

943 expressing transgenics in the wild-type (pink triangles, orange squares), and in NLP-7 over-

944 expressing transgenics in the *goa-1(n1134)* (pink open triangles) and *goa-1(sa734)* null mutant

945 background (orange open squares). Data in orange squares are from animals that also carry the

946 *vsIs183* transgene used for HSN Ca^{2+} imaging. Error bars indicate 95% confidence intervals for

947 the mean. Asterisk indicates p<0.0001 (One-Way ANOVA with Bonferroni correction for multiple

948 comparisons). N≥30 animals for each strain (**B**) Measure of hyperactive egg laying in wild-type

949 (black), *goa-1(sa734)* null mutants (blue), and *goa-1(sa734)* null mutants over-expressing NLP-

bioRxiv preprint doi: https://doi.org/10.1101/701664; this version posted July 13, 2019. The copyright holder for this preprint (which was not certified by peer review) is the author/funder, who has granted bioRxiv a license to display the preprint in perpetuity. It is made available under aCC-BY 4.0 International license.

7 neuropeptides (orange). Both *goa-1(sa734)* mutant strains also carry the *vsIs183* transgene used for HSN Ca^{2+} imaging. (**C**) NLP-7 over-expression silences HSN Ca^{2+} activity. Representative GCaMP5/mCherry ratio traces showing HSN Ca^{2+} activity in wild-type (black), *goa-1(sa734)* null mutants, and NLP-7 overexpressing transgenic animals in the wild-type (pink) and *goa-1(sa734)* null mutant backgrounds (orange). Arrowheads indicate egg-laying events **(D)** Scatter plots show HSN Ca^{2+} peaks per minute measurements for each individual in wild type (black), *goa-1(sa734)* null mutants, and NLP-7 over-expressing animals in the wild-type (pink) and *goa-1(sa734)* null mutant backgrounds (orange). Error bars indicate 95% confidence intervals for the mean for N≥10 animals; asterisk indicates p≤0.0001, pound sign indicates p≤0.0007, and n.s. indicates p>0.05 (one-way ANOVA with Bonferroni correction for multiple comparisons).

bioRxiv preprint doi: https://doi.org/10.1101/701664; this version posted July 13, 2019. The copyright holder for this preprint (which was not certified by peer review) is the author/funder, who has granted bioRxiv a license to display the preprint in perpetuity. It is made available under aCC-BY 4.0 International license.

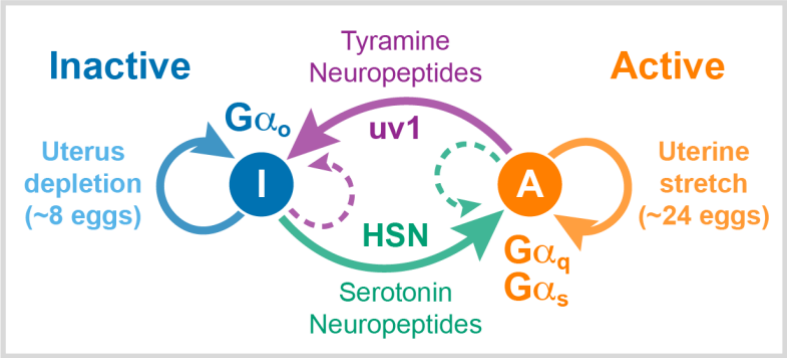

Figure 7. Model for how Gαo signaling acts to inhibit HSN neurotransmitter release and prolong the egg-laying inactive state. Serotonin and NLP-3 neuropeptides released from HSN (filled green arrow) signal through excitatory receptors coupled to $G\alpha_q$ and $G\alpha_s$ to promote vulval muscle electrical excitability and the egg-laying active state (A). Feedback of egg accumulation in the uterus maintains the active state (filled orange arrow). Retrograde feedback of ongoing vulval muscle Ca^{2+} activity (dashed green arrow) also drives burst firing in the HSNs which further maintains the circuit in the active state. Egg release mechanically activates the uv1 neuroendocrine cells which release tyramine, NLP-7, and FLP-11 neuropeptides (filled purple arrow) which signal through inhibitory receptors and $G\alpha_o$ to promote the inactive state (I). Not shown are other inhibitory neuropeptides released from sensory neurons in response to aversive environmental conditions that also signal to activate inhibitory receptors and $G\alpha_o$. Feedback of egg depletion from the uterus maintains the inactive state (filled blue arrow). Vulval openings that fail to release eggs may feedback and prolong Ca^{2+} signaling in the uv1 cells and VC neurons (dashed purple arrow) which further signal to reduce the probability of the circuit leaving the inactive state.

bioRxiv preprint doi: https://doi.org/10.1101/701664; this version posted July 13, 2019. The copyright holder for this preprint (which was not certified by peer review) is the author/funder, who has granted bioRxiv a license to display the preprint in perpetuity. It is made available under aCC-BY 4.0 International license.

Video 1. GCaMP5:mCherry ratio recording of HSN Ca^{2+} activity in a control, wild-type adult animal during an egg-laying active state. High Ca^{2+} is indicated in red while low calcium is in blue. Head is at left, tail is at right.

Video 2. GCaMP5:mCherry ratio recording of HSN Ca^{2+} activity in a *goa-1(n1134)* mutant adult animal during an egg-laying active state. High Ca^{2+} is indicated in red while low calcium is in blue. Head is at left, tail is at right.

Video 3. GCaMP5:mCherry ratio recording of HSN Ca^{2+} activity in a *goa-1(sa734)* null mutant adult animal during an egg-laying active state. High Ca^{2+} is indicated in red while low calcium is in blue. Head is at right, tail is at left.

Video 4. GCaMP5:mCherry ratio recording of HSN Ca^{2+} activity in an wild-type adult animal during an egg-laying active state. High Ca^{2+} is indicated in red while low calcium is in blue. Head is at top, tail is at bottom.

Video 5. GCaMP5:mCherry ratio recording of HSN Ca^{2+} activity in a transgenic adult animal expressing Pertussis Toxin in the HSNs from the *tph-1* gene promoter during an egg-laying active state. High Ca^{2+} is indicated in red while low calcium is in blue. Head is at top, tail is at bottom.

Video 6. GCaMP5:mCherry ratio recording of vulval muscle Ca^{2+} activity in a control wild-type adult animal during an egg-laying active state. High Ca^{2+} is indicated in red while low calcium is in blue. Head is at right, tail is at top.

Video 7. GCaMP5:mCherry ratio recording of vulval muscle Ca^{2+} activity in a *goa-1(n1134)* mutant adult animal during an egg-laying active state. High Ca^{2+} is indicated in red while low calcium is in blue. Head is at right, tail is at left.

bioRxiv preprint doi: https://doi.org/10.1101/701664; this version posted July 13, 2019. The copyright holder for this preprint (which was not certified by peer review) is the author/funder, who has granted bioRxiv a license to display the preprint in perpetuity. It is made available under aCC-BY 4.0 International license.

Video 8. GCaMP5:mCherry ratio recording of vulval muscle Ca^{2+} activity in a control wild-type adult animal during an egg-laying active state. High Ca^{2+} is indicated in red while low calcium is in blue. Head is at top, tail is at bottom.

Video 9. GCaMP5:mCherry ratio recording of vulval muscle Ca^{2+} activity in a transgenic adult animal expressing Pertussis Toxin in the HSNs from the *tph-1* gene promoter during an egg-laying active state. High Ca^{2+} is indicated in red while low calcium is in blue. Head is at left, tail is at right.

bioRxiv preprint doi: https://doi.org/10.1101/701664; this version posted July 13, 2019. The copyright holder for this preprint (which was not certified by peer review) is the author/funder, who has granted bioRxiv a license to display the preprint in perpetuity. It is made available under aCC-BY 4.0 International license.

1018 ***Table 2.*** *Strain names and genotypes for all animals used in this study (behavior assays and*

1019 *calcium imaging)*

1020

Strain	Feature	Genotype	Reference
LX1832	Strain for transgene production, blue-light insensitive, multi-vulva at 20°C in the absence of *lin-15(+)* rescue transgene.	*lite-1(ce314) lin-15(n765ts) X*	(Gurel et al., 2012)
N2	Bristol wild-type strain	wild type	(Brenner, 1974)
LX2004	HSN GCaMP5, mCherry	*vsIs183 lite-1(ce314) lin-15(n765ts) X*	(Collins et al., 2016)
LX1918	vulval muscle GCaMP5, mCherry	*vsIs164 lite-1(ce314) lin-15(n765ts) X*	(Collins et al., 2016)
MT2426	*goa-1(Gα$_o$)* reduced-function mutant, hyperactive egg laying	*goa-1(n1134) I*	(Segalat et al., 1995)
DG1856	*goa-1(Gα$_o$)* null mutant, hyperactive egg laying	*goa-1(sa734) I*	(Robatzek and Thomas, 2000)
LX850	HSN and NSM Pertussis Toxin, hyperactive egg laying	*vsIs50; lin-15(n765ts)*	(Tanis et al., 2008)
LX849	HSN and NSM activated GOA-1(Q205L), egg laying defective	*vsIs49; lin-15(n765ts)*	(Tanis et al., 2008)
MT8504	Increased Gα$_o$ signaling due to mutation in RGS protein, EGL-10	*egl-10(md176)*	(Koelle and Horvitz, 1996)
MIA220	*goa-1(Gα$_o$)* reduced-function mutant in *lite-1(ce314), lin-15(n765ts)* background to facilitate strain construction, hyperactive egg laying	*goa-1(n1134) I; lite-1(ce314) lin-15(n765ts) X*	this study
MIA210	*goa-1(Gα$_o$)* reduced-function mutant; HSN GCaMP, mCherry	*goa-1(n1134) I; vsIs183 lite-1(ce314) lin-15(n765ts) X*	this study
MIA263	*goa-1(Gα$_o$)* null mutant; HSN GCaMP5, mCherry	*goa-1(sa734) I; vsIs183 lite-1(ce314) lin-15(n765ts) X*	this study
MIA216	Increased Gα$_o$ signaling; HSN GCaMP5, mCherry	*egl-10(md176) V; vsIs183 lite-1(ce314) lin-15(n765ts) X*	this study
MIA277	Increased Gα$_o$ signaling in HSN; HSN GCaMP5, mCherry	*vsIs49/+, +/vsIs183 lite-1(ce314) lin-15(n765ts) X (trans-heterozygote)*	this study
LX2007	HSN GCaMP5, mCherry	*vsIs186 lite-1(ce314) lin-15(n765ts) X*	(Collins et al., 2016)

bioRxiv preprint doi: https://doi.org/10.1101/701664; this version posted July 13, 2019. The copyright holder for this preprint (which was not certified by peer review) is the author/funder, who has granted bioRxiv a license to display the preprint in perpetuity. It is made available under aCC-BY 4.0 International license.

MIA218	HSN and NSM Pertussis Toxin in blue-light insensitive, *lin-15* multi-vulva background	*vsIs50 lite-1(ce314) lin-15(n765ts) X*	this study
MIA227	HSN and NSM Pertussis Toxin; HSN GCaMP5, mCherry	*vsIs186; vsIs50 lite-1(ce314) lin-15(n765ts) X*	this study
MIA214	*goa-1(Gα$_o$)* reduced-function mutant; vulval muscle GCaMP5, mCherry	*goa-1(n1134) I; vsIs164 lite-1(ce314) lin-15(n765ts) X*	this study
LX1919	Vulval muscle GCaMP5, mCherry	*vsIs165; lite-1(ce314) lin-15(n765ts) X*	(Collins et al., 2016)
MIA245	*goa-1(Gα$_o$)* null-function mutant; vulval muscle GCaMP5, mCherry	*vsIs50 X vsIs165; lite-1(ce314) lin-15(n765ts) X*	this study
MIA295	*goa-1(Gα$_o$)* null mutant, vulval muscles GCaMP, mCherry	*goa-1(sa734) I; vsIs164 lite-1(ce314) lin-15(n765ts) X*	this study
MIA291	Increased Gα$_o$ signaling in HSN; HSN GCaMP5, mCherry	*vsIs49; vsIs165 lite-1(ce314) lin-15(n765ts) X*	this study
MIA290	Increased Gα$_o$ signaling; vulval muscle GCaMP5, mCherry	*egl-10(md176) V; vsIs183 lite-1(ce314) lin-15(n765ts) X*	this study
MIA256	Vulval muscle mCherry (*ceh-24* promoter)	*keyEx45; lite-1(ce314) lin-15(n765ts) X*	this study
MIA257	Vulval muscle mCherry + Pertussis Toxin (*ceh-24* promoter)	*keyEx46; lite-1(ce314) lin-15(n765ts) X*	this study
MIA258	Vulval muscle mCherry + Activated GOA-1(Q205L) (*ceh-24* promoter)	*keyEx47; lite-1(ce314) lin-15(n765ts) X*	this study
MIA262	Vulval muscle mCherry + Tetanus toxin (*ceh-24* promoter)	*keyEx51*; *lite-1(ce314) lin-15(n765ts)*	this study
MIA259	uv1 cells mCherry (*tdc-1* promoter, *ocr-2* 3' UTR)	*keyEx48; lite-1(ce314) lin-15(n765ts) X*	this study
MIA260	uv1 cells mCherry + Pertussis Toxin (*tdc-1* promoter, *ocr-2* 3' UTR)	*keyEx49; lite-1(ce314) lin-15(n765ts) X*	this study
MIA261	uv1 cells mCherry + Activated GOA-1(Q205L) (*tdc-1* promoter, *ocr-2* 3' UTR)	*keyEx50; lite-1(ce314) lin-15(n765ts) X*	this study
MIA278	HSN/NSM *gpb-1* and *gpc-2* overexpression + GFP (*tph-1* promoter)	*keyEx52; lite-1(ce314) lin-15(n765ts) X*	this study
MIA279	HSN/NSM empty + GFP (*tph-1* promoter)	*keyEx53; lite-1(ce314) lin-15(n765ts) X*	this study
KG421	GSA-1(Gα$_s$) gain-of-function mutant. Hyperactive locomotion	*gsa-1(ce81) I*	(Schade et al., 2005)
MT1073	EGL-4 (Protein Kinase G) null mutant. Egg-laying defective, roaming locomotion	*egl-4(n479) IV*	(L'Etoile et al., 2002)

bioRxiv preprint doi: https://doi.org/10.1101/701664; this version posted July 13, 2019. The copyright holder for this preprint (which was not certified by peer review) is the author/funder, who has granted bioRxiv a license to display the preprint in perpetuity. It is made available under aCC-BY 4.0 International license.

MT1074	EGL-4 (Protein Kinase G) loss-of-function mutant. Egg-laying defective, roaming locomotion	*egl-4(n478) IV*	(L'Etoile et al., 2002)
DA521	EGL-4 (Protein Kinase G) gain-of-function mutant. Hyperactive egg laying, sluggish locomotion	*egl-4(ad805) IV*	(Raizen et al., 2006)
MIA36	EGL-4 (Protein Kinase G) gain-of-function mutant. Hyperactive egg laying, sluggish locomotion	*egl-4(mg410) IV*	(Hao et al., 2011)
KG518	ACY-1 (Adenylate Cyclase) gain-of-function mutant. Hyperactive locomotion	*acy-1(ce2) III*	(Schade et al., 2005)
KG532	KIN-2 (Protein Kinase A inhibitory regulatory subunit) loss-of-function mutant. Hypersensitive to stimuli	*kin-2(ce179) X*	(Schade et al., 2005)
KG744	PDE-4 (phosphodiesterase) loss-of-function mutant, Hyperactive locomotion	*pde-4(ce268) II*	(Charlie et al., 2006b)
MIA282	PDE-2 (phosphodiesterase) loss-of-function mutant	*pde-2(qj6)*	(Fujiwara et al., 2015)
MIA293	NLP-7 overexpression; HSN GCaMP5, mCherry	*ufIs118; vsIs183 lite-1(ce314) lin-15(n765ts) X*	(Banerjee et al., 2017) & this study
MIA294	NLP-7 overexpression; *goa-1(Gα$_o$)* null mutant; HSN GCaMP5, mCherry	*ufIs118; goa-1(sa734) I; vsIs183 lite-1(ce314) lin-15(n765ts) X*	(Banerjee et al., 2017) & this study

1021

bioRxiv preprint doi: https://doi.org/10.1101/701664; this version posted July 13, 2019. The copyright holder for this preprint (which was not certified by peer review) is the author/funder, who has granted bioRxiv a license to display the preprint in perpetuity. It is made available under aCC-BY 4.0 International license.

References

Alkema MJ, Hunter-Ensor M, Ringstad N, Horvitz HR (2005) Tyramine Functions independently of octopamine in the Caenorhabditis elegans nervous system. Neuron 46:247-260.

Banerjee N, Bhattacharya R, Gorczyca M, Collins KM, Francis MM (2017) Local neuropeptide signaling modulates serotonergic transmission to shape the temporal organization of *C. elegans* egg-laying behavior. PLoS Genet 13:e1006697.

Bastiani CA, Gharib S, Simon MI, Sternberg PW (2003) Caenorhabditis elegans Galphaq regulates egg-laying behavior via a PLCbeta-independent and serotonin-dependent signaling pathway and likely functions both in the nervous system and in muscle. Genetics 165:1805-1822.

Bellemer A, Hirata T, Romero MF, Koelle MR (2011) Two types of chloride transporters are required for GABA(A) receptor-mediated inhibition in *C. elegans*. EMBO J 30:1852-1863.

Brenner S (1974) The genetics of *Caenorhabditis elegans*. Genetics 77:71-94.

Brewer JC, Collins KM, Koelle MR, Olsen A (2019) Serotonin and neuropeptides are both released by the HSN command neuron to initiate C. elegans egg laying. PLoS Genet 15.

Brundage L, Avery L, Katz A, Kim UJ, Mendel JE, Sternberg PW, Simon MI (1996) Mutations in a C. elegans Gqalpha gene disrupt movement, egg laying, and viability. Neuron 16:999-1009.

Carnell L, Illi J, Hong SW, McIntire SL (2005) The G-protein-coupled serotonin receptor SER-1 regulates egg laying and male mating behaviors in *Caenorhabditis elegans*. J Neurosci 25:10671-10681.

Charlie NK, Thomure AM, Schade MA, Miller KG (2006a) The Dunce cAMP phosphodiesterase PDE-4 negatively regulates G alpha(s)-dependent and G alpha(s)-independent cAMP pools in the Caenorhabditis elegans synaptic signaling network. Genetics 173:111-130.

Charlie NK, Schade MA, Thomure AM, Miller KG (2006b) Presynaptic UNC-31 (CAPS) is required to activate the G alpha(s) pathway of the Caenorhabditis elegans synaptic signaling network. Genetics 172:943-961.

Chase DL, Pepper JS, Koelle MR (2004) Mechanism of extrasynaptic dopamine signaling in *Caenorhabditis elegans*. Nat Neurosci 7:1096-1103.

Chew YL, Grundy LJ, Brown AEX, Beets I, Schafer WR (2018) Neuropeptides encoded by nlp-49 modulate locomotion, arousal and egg-laying behaviours in Caenorhabditis elegans via the receptor SEB-3. Philos Trans R Soc Lond B Biol Sci 373.

Clancy SM, Fowler CE, Finley M, Suen KF, Arrabit C, Berton F, Kosaza T, Casey PJ, Slesinger PA (2005) Pertussis-toxin-sensitive Galpha subunits selectively bind to C-terminal domain of neuronal GIRK channels: evidence for a heterotrimeric G-protein-channel complex. Mol Cell Neurosci 28:375-389.

Coleman B, Topalidou I, Ailion M (2018) Modulation of Gq-Rho Signaling by the ERK MAPK Pathway Controls Locomotion in Caenorhabditis elegans. Genetics 209:523-535.

Collins KM, Koelle MR (2013) Postsynaptic ERG potassium channels limit muscle excitability to allow distinct egg-laying behavior states in *Caenorhabditis elegans*. J Neurosci 33:761-775.

Collins KM, Bode A, Fernandez RW, Tanis JE, Brewer JC, Creamer MS, Koelle MR (2016) Activity of the *C. elegans* egg-laying behavior circuit is controlled by competing activation and feedback inhibition. Elife 5:e21126.

Desai C, Garriga G, McIntire SL, Horvitz HR (1988) A genetic pathway for the development of the Caenorhabditis elegans HSN motor neurons. Nature 336:638-646.

bioRxiv preprint doi: https://doi.org/10.1101/701664; this version posted July 13, 2019. The copyright holder for this preprint (which was not certified by peer review) is the author/funder, who has granted bioRxiv a license to display the preprint in perpetuity. It is made available under aCC-BY 4.0 International license.

Dong MQ, Chase D, Patikoglou GA, Koelle MR (2000) Multiple RGS proteins alter neural G protein signaling to allow C. elegans to rapidly change behavior when fed. Genes Dev 14:2003-2014.

Emtage L, Aziz-Zaman S, Padovan-Merhar O, Horvitz HR, Fang-Yen C, Ringstad N (2012) IRK-1 potassium channels mediate peptidergic inhibition of *Caenorhabditis elegans* serotonin neurons via a G(o) signaling pathway. J Neurosci 32:16285-16295.

Fenk LA, de Bono M (2015) Environmental CO2 inhibits Caenorhabditis elegans egg-laying by modulating olfactory neurons and evokes widespread changes in neural activity. Proc Natl Acad Sci U S A 112:E3525-3534.

Flavell SW, Pokala N, Macosko EZ, Albrecht DR, Larsch J, Bargmann CI (2013) Serotonin and the neuropeptide PDF initiate and extend opposing behavioral states in *C. elegans*. Cell 154:1023-1035.

Fujiwara M, Sengupta P, McIntire SL (2002) Regulation of body size and behavioral state of C. elegans by sensory perception and the EGL-4 cGMP-dependent protein kinase. Neuron 36:1091-1102.

Fujiwara M, Hino T, Miyamoto R, Inada H, Mori I, Koga M, Miyahara K, Ohshima Y, Ishihara T (2015) The Importance of cGMP Signaling in Sensory Cilia for Body Size Regulation in Caenorhabditis elegans. Genetics 201:1497-1510.

Gallagher T, Kim J, Oldenbroek M, Kerr R, You YJ (2013) ASI regulates satiety quiescence in C. elegans. J Neurosci 33:9716-9724.

Gao S, Zhen M (2011) Action potentials drive body wall muscle contractions in Caenorhabditis elegans. Proc Natl Acad Sci U S A 108:2557-2562.

Ghil S, Choi JM, Kim SS, Lee YD, Liao Y, Birnbaumer L, Suh-Kim H (2006) Compartmentalization of protein kinase A signaling by the heterotrimeric G protein Go. Proc Natl Acad Sci U S A 103:19158-19163.

Goulding EH, Schenk AK, Juneja P, MacKay AW, Wade JM, Tecott LH (2008) A robust automated system elucidates mouse home cage behavioral structure. Proc Natl Acad Sci U S A 105:20575-20582.

Gruninger TR, Gualberto DG, Garcia LR (2008) Sensory perception of food and insulin-like signals influence seizure susceptibility. PLoS Genet 4:e1000117.

Gruninger TR, Gualberto DG, LeBoeuf B, Garcia LR (2006) Integration of male mating and feeding behaviors in Caenorhabditis elegans. J Neurosci 26:169-179.

Gurel G, Gustafson MA, Pepper JS, Horvitz HR, Koelle MR (2012) Receptors and other signaling proteins required for serotonin control of locomotion in *Caenorhabditis elegans*. Genetics 192:1359-1371.

Hallem EA, Spencer WC, McWhirter RD, Zeller G, Henz SR, Ratsch G, Miller DM, 3rd, Horvitz HR, Sternberg PW, Ringstad N (2011) Receptor-type guanylate cyclase is required for carbon dioxide sensation by Caenorhabditis elegans. Proc Natl Acad Sci U S A 108:254-259.

Hao Y, Xu N, Box AC, Schaefer L, Kannan K, Zhang Y, Florens L, Seidel C, Washburn MP, Wiegraebe W, Mak HY (2011) Nuclear cGMP-dependent kinase regulates gene expression via activity-dependent recruitment of a conserved histone deacetylase complex. PLoS Genet 7:e1002065.

Harfe BD, Fire A (1998) Muscle and nerve-specific regulation of a novel NK-2 class homeodomain factor in *Caenorhabditis elegans*. Development 125:421-429.

Herlitze S, Garcia DE, Mackie K, Hille B, Scheuer T, Catterall WA (1996) Modulation of Ca2+ channels by G-protein beta gamma subunits. Nature 380:258-262.

Hille B (1994) Modulation of ion-channel function by G-protein-coupled receptors. Trends Neurosci 17:531-536.

bioRxiv preprint doi: https://doi.org/10.1101/701664; this version posted July 13, 2019. The copyright holder for this preprint (which was not certified by peer review) is the author/funder, who has granted bioRxiv a license to display the preprint in perpetuity. It is made available under aCC-BY 4.0 International license.

Hobson RJ, Hapiak VM, Xiao H, Buehrer KL, Komuniecki PR, Komuniecki RW (2006) SER-7, a *Caenorhabditis elegans* 5-HT7-like receptor, is essential for the 5-HT stimulation of pharyngeal pumping and egg laying. Genetics 172:159-169.

Iwanir S, Brown AS, Nagy S, Najjar D, Kazakov A, Lee KS, Zaslaver A, Levine E, Biron D (2016) Serotonin promotes exploitation in complex environments by accelerating decision-making. BMC Biol 14:9.

Jiang M, Spicher K, Boulay G, Wang Y, Birnbaumer L (2001) Most central nervous system D2 dopamine receptors are coupled to their effectors by Go. Proc Natl Acad Sci U S A 98:3577-3582.

Jose AM, Bany IA, Chase DL, Koelle MR (2007) A specific subset of transient receptor potential vanilloid-type channel subunits in Caenorhabditis elegans endocrine cells function as mixed heteromers to promote neurotransmitter release. Genetics 175:93-105.

Kobayashi I, Shibasaki H, Takahashi K, Tohyama K, Kurachi Y, Ito H, Ui M, Katada T (1990) Purification and characterization of five different alpha subunits of guanine-nucleotide-binding proteins in bovine brain membranes. Their physiological properties concerning the activities of adenylate cyclase and atrial muscarinic K+ channels. Eur J Biochem 191:499-506.

Koelle MR (2016) Neurotransmitter signaling through heterotrimeric G proteins: insights from studies in C. elegans. WormBook:1-78.

Koelle MR, Horvitz HR (1996) EGL-10 regulates G protein signaling in the C. elegans nervous system and shares a conserved domain with many mammalian proteins. Cell 84:115-125.

L'Etoile ND, Coburn CM, Eastham J, Kistler A, Gallegos G, Bargmann CI (2002) The cyclic GMP-dependent protein kinase EGL-4 regulates olfactory adaptation in C. elegans. Neuron 36:1079-1089.

Lackner MR, Nurrish SJ, Kaplan JM (1999) Facilitation of synaptic transmission by EGL-30 Gqalpha and EGL-8 PLCbeta: DAG binding to UNC-13 is required to stimulate acetylcholine release. Neuron 24:335-346.

Laine V, Segor JR, Zhan H, Bessereau JL, Jospin M (2014) Hyperactivation of L-type voltage-gated Ca2+ channels in Caenorhabditis elegans striated muscle can result from point mutations in the IS6 or the IIIS4 segment of the alpha1 subunit. J Exp Biol 217:3805-3814.

LeBoeuf B, Gruninger TR, Garcia LR (2007) Food deprivation attenuates seizures through CaMKII and EAG K+ channels. PLoS Genet 3:1622-1632.

Lee KS, Iwanir S, Kopito RB, Scholz M, Calarco JA, Biron D, Levine E (2017) Serotonin-dependent kinetics of feeding bursts underlie a graded response to food availability in C. elegans. Nat Commun 8:14221.

Lee RY, Lobel L, Hengartner M, Horvitz HR, Avery L (1997) Mutations in the alpha1 subunit of an L-type voltage-activated Ca2+ channel cause myotonia in Caenorhabditis elegans. EMBO J 16:6066-6076.

Li P, Collins KM, Koelle MR, Shen K (2013) LIN-12/Notch signaling instructs postsynaptic muscle arm development by regulating UNC-40/DCC and MADD-2 in *Caenorhabditis elegans*. Elife 2:e00378.

Liu P, Ge Q, Chen B, Salkoff L, Kotlikoff MI, Wang ZW (2011) Genetic dissection of ion currents underlying all-or-none action potentials in C. elegans body-wall muscle cells. J Physiol 589:101-117.

Liu Q, Kidd PB, Dobosiewicz M, Bargmann CI (2018) C. elegans AWA Olfactory Neurons Fire Calcium-Mediated All-or-None Action Potentials. Cell 175:57-70 e17.

Lopez-Cruz A, Sordillo A, Pokala N, Liu Q, McGrath PT, Bargmann CI (2019) Parallel Multimodal Circuits Control an Innate Foraging Behavior. Neuron 102:407-419 e408.

bioRxiv preprint doi: https://doi.org/10.1101/701664; this version posted July 13, 2019. The copyright holder for this preprint (which was not certified by peer review) is the author/funder, who has granted bioRxiv a license to display the preprint in perpetuity. It is made available under aCC-BY 4.0 International license.

Lutas A, Lahmann C, Soumillon M, Yellen G (2016) The leak channel NALCN controls tonic firing and glycolytic sensitivity of substantia nigra pars reticulata neurons. Elife 5.

Marder E (2012) Neuromodulation of neuronal circuits: back to the future. Neuron 76:1-11.

Mase Y, Yokogawa M, Osawa M, Shimada I (2012) Structural basis for modulation of gating property of G protein-gated inwardly rectifying potassium ion channel (GIRK) by i/o-family G protein alpha subunit (Galphai/o). J Biol Chem 287:19537-19549.

Mathews EA, Garcia E, Santi CM, Mullen GP, Thacker C, Moerman DG, Snutch TP (2003) Critical residues of the Caenorhabditis elegans unc-2 voltage-gated calcium channel that affect behavioral and physiological properties. J Neurosci 23:6537-6545.

Matsubara H (2002) [Angiotensin II type 2 (AT2) receptor signal and cardiovascular action]. Nihon Yakurigaku Zasshi 119:95-102.

Mendel JE, Korswagen HC, Liu KS, Hajdu-Cronin YM, Simon MI, Plasterk RH, Sternberg PW (1995) Participation of the protein Go in multiple aspects of behavior in C. elegans. Science 267:1652-1655.

Miller KG, Emerson MD, Rand JB (1999) Goalpha and diacylglycerol kinase negatively regulate the Gqalpha pathway in C. elegans. Neuron 24:323-333.

Moresco JJ, Koelle MR (2004) Activation of EGL-47, a Galpha(o)-coupled receptor, inhibits function of hermaphrodite-specific motor neurons to regulate *Caenorhabditis elegans* egg-laying behavior. J Neurosci 24:8522-8530.

Mumby SM, Heukeroth RO, Gordon JI, Gilman AG (1990) G-protein alpha-subunit expression, myristoylation, and membrane association in COS cells. Proc Natl Acad Sci U S A 87:728-732.

Nakamura K et al. (2013) De Novo mutations in GNAO1, encoding a Galphao subunit of heterotrimeric G proteins, cause epileptic encephalopathy. Am J Hum Genet 93:496-505.

Nurrish S, Segalat L, Kaplan JM (1999) Serotonin inhibition of synaptic transmission: Galpha(0) decreases the abundance of UNC-13 at release sites. Neuron 24:231-242.

Peleg S, Varon D, Ivanina T, Dessauer CW, Dascal N (2002) G(alpha)(i) controls the gating of the G protein-activated K(+) channel, GIRK. Neuron 33:87-99.

Qin N, Platano D, Olcese R, Stefani E, Birnbaumer L (1997) Direct interaction of gbetagamma with a C-terminal gbetagamma-binding domain of the Ca2+ channel alpha1 subunit is responsible for channel inhibition by G protein-coupled receptors. Proc Natl Acad Sci U S A 94:8866-8871.

Raizen DM, Cullison KM, Pack AI, Sundaram MV (2006) A novel gain-of-function mutant of the cyclic GMP-dependent protein kinase egl-4 affects multiple physiological processes in Caenorhabditis elegans. Genetics 173:177-187.

Ravi B, Garcia J, Collins KM (2018a) Homeostatic feedback modulates the development of two-state patterned activity in a model serotonin motor circuit in Caenorhabditis elegans. J Neurosci 38:6283-6298.

Ravi B, Nassar LM, Kopchock RJ, 3rd, Dhakal P, Scheetz M, Collins KM (2018b) Ratiometric calcium imaging of individual neurons in behaving Caenorhabditis elegans. J Vis Exp.

Reuveny E, Slesinger PA, Inglese J, Morales JM, Iniguez-Lluhi JA, Lefkowitz RJ, Bourne HR, Jan YN, Jan LY (1994) Activation of the cloned muscarinic potassium channel by G protein beta gamma subunits. Nature 370:143-146.

Ringstad N, Horvitz HR (2008) FMRFamide neuropeptides and acetylcholine synergistically inhibit egg-laying by *C. elegans*. Nat Neurosci 11:1168-1176.

Robatzek M, Thomas JH (2000) Calcium/calmodulin-dependent protein kinase II regulates Caenorhabditis elegans locomotion in concert with a G(o)/G(q) signaling network. Genetics 156:1069-1082.

bioRxiv preprint doi: https://doi.org/10.1101/701664; this version posted July 13, 2019. The copyright holder for this preprint (which was not certified by peer review) is the author/funder, who has granted bioRxiv a license to display the preprint in perpetuity. It is made available under aCC-BY 4.0 International license.

Schade MA, Reynolds NK, Dollins CM, Miller KG (2005) Mutations that rescue the paralysis of Caenorhabditis elegans ric-8 (synembryn) mutants activate the G alpha(s) pathway and define a third major branch of the synaptic signaling network. Genetics 169:631-649.

Schafer WR, Kenyon CJ (1995) A calcium-channel homologue required for adaptation to dopamine and serotonin in Caenorhabditis elegans. Nature 375:73-78.

Scholz M, Dinner AR, Levine E, Biron D (2017) Stochastic feeding dynamics arise from the need for information and energy. Proc Natl Acad Sci U S A 114:9261-9266.

Segalat L, Elkes DA, Kaplan JM (1995) Modulation of serotonin-controlled behaviors by Go in *Caenorhabditis elegans*. Science 267:1648-1651.

Tanis JE, Moresco JJ, Lindquist RA, Koelle MR (2008) Regulation of serotonin biosynthesis by the G proteins Galphao and Galphaq controls serotonin signaling in *Caenorhabditis elegans*. Genetics 178:157-169.

Tanis JE, Bellemer A, Moresco JJ, Forbush B, Koelle MR (2009) The potassium chloride cotransporter KCC-2 coordinates development of inhibitory neurotransmission and synapse structure in *Caenorhabditis elegans*. J Neurosci 29:9943-9954.

Topalidou I, Cooper K, Pereira L, Ailion M (2017a) Dopamine negatively modulates the NCA ion channels in C. elegans. PLoS Genet 13:e1007032.

Topalidou I, Chen PA, Cooper K, Watanabe S, Jorgensen EM, Ailion M (2017b) The NCA-1 and NCA-2 Ion Channels Function Downstream of Gq and Rho To Regulate Locomotion in Caenorhabditis elegans. Genetics 206:265-282.

Trent C, Tsuing N, Horvitz HR (1983) Egg-laying defective mutants of the nematode Caenorhabditis elegans. Genetics 104:619-647.

Tsai EJ, Kass DA (2009) Cyclic GMP signaling in cardiovascular pathophysiology and therapeutics. Pharmacol Ther 122:216-238.

Waggoner LE, Zhou GT, Schafer RW, Schafer WR (1998) Control of alternative behavioral states by serotonin in Caenorhabditis elegans. Neuron 21:203-214.

White JG, Southgate E, Thomson JN, Brenner S (1986) The structure of the nervous system of the nematode *Caenorhabditis elegans*. Philos Trans R Soc Lond B Biol Sci 314:1-340.

Williams SL, Lutz S, Charlie NK, Vettel C, Ailion M, Coco C, Tesmer JJ, Jorgensen EM, Wieland T, Miller KG (2007) Trio's Rho-specific GEF domain is the missing Galpha q effector in C. elegans. Genes Dev 21:2731-2746.

Xiao H, Hapiak VM, Smith KA, Lin L, Hobson RJ, Plenefisch J, Komuniecki R (2006) SER-1, a *Caenorhabditis elegans* 5-HT2-like receptor, and a multi-PDZ domain containing protein (MPZ-1) interact in vulval muscle to facilitate serotonin-stimulated egg-laying. Dev Biol 298:379-391.

Yamada K, Hirotsu T, Matsuki M, Kunitomo H, Iino Y (2009) GPC-1, a G protein gamma-subunit, regulates olfactory adaptation in Caenorhabditis elegans. Genetics 181:1347-1357.

Yeh E, Ng S, Zhang M, Bouhours M, Wang Y, Wang M, Hung W, Aoyagi K, Melnik-Martinez K, Li M, Liu F, Schafer WR, Zhen M (2008) A putative cation channel, NCA-1, and a novel protein, UNC-80, transmit neuronal activity in *C. elegans*. PLoS Biol 6:e55.

You YJ, Kim J, Raizen DM, Avery L (2008) Insulin, cGMP, and TGF-beta signals regulate food intake and quiescence in C. elegans: a model for satiety. Cell Metab 7:249-257.

Yue X, Zhao J, Li X, Fan Y, Duan D, Zhang X, Zou W, Sheng Y, Zhang T, Yang Q, Luo J, Duan S, Xiao R, Kang L (2018) TMC Proteins Modulate Egg Laying and Membrane Excitability through a Background Leak Conductance in C. elegans. Neuron 97:571-585 e575.

Zang KE, Ho E, Ringstad N (2017) Inhibitory peptidergic modulation of *C. elegans* serotonin neurons is gated by T-type calcium channels. Elife 6:e22771.

bioRxiv preprint doi: https://doi.org/10.1101/701664; this version posted July 13, 2019. The copyright holder for this preprint (which was not certified by peer review) is the author/funder, who has granted bioRxiv a license to display the preprint in perpetuity. It is made available under aCC-BY 4.0 International license.

Zhang J, Pratt RE (1996) The AT2 receptor selectively associates with Gialpha2 and Gialpha3 in the rat fetus. J Biol Chem 271:15026-15033.

Zhang M, Chung SH, Fang-Yen C, Craig C, Kerr RA, Suzuki H, Samuel AD, Mazur E, Schafer WR (2008) A self-regulating feed-forward circuit controlling C. elegans egg-laying behavior. Curr Biol 18:1445-1455.

Zou W, Fu J, Zhang H, Du K, Huang W, Yu J, Li S, Fan Y, Baylis HA, Gao S, Xiao R, Ji W, Kang L, Xu T (2018) Decoding the intensity of sensory input by two glutamate receptors in one C. elegans interneuron. Nat Commun 9:4311.